Angewandte Chemie
Eine Zeitschrift der Gesellschaft Deutscher Chemiker

Supporting Information

Injury-Triggered Blueing Reactions of *Psilocybe* "Magic" Mushrooms

Claudius Lenz[+], *Jonas Wick*[+], *Daniel Braga, María García-Altares, Gerald Lackner, Christian Hertweck, Markus Gressler, and Dirk Hoffmeister**

anie_201910175_sm_miscellaneous_information.pdf
anie_201910175_sm_Movie.avi
anie_201910175_sm_Movie_1_s.avi

SUPPORTING INFORMATION

Table of Contents

Experimental procedures. 2
Table S1. Peptide mass fingerprinting of the phosphatase-containing protein fraction 9
Table S2. Characteristics of biosynthetic genes *psiP* and *psiL* 11
Table S3. Predicted subcellular localization of PsiP and PsiL.. 12
Table S4. PsiP-like enzymes in psilocybin-producing mushrooms and *Coprinopsis cinerea*. 13
Table S5. Peptide mass fingerprinting of the oxidase-containing protein fraction 14
Table S6. PsiL-like enzymes in other psilocybin-producing mushrooms 16
Table S7. Comparison of laccase activity 16
Table S8. Psilocyl oligomers observed by mass spectrometry 17
Figure S1. Size exclusion chromatograms of the FPLC purification cascade for PsiP 19
Figure S2. Peptide mass fingerprinting of phosphatase 20
Figure S3. Signal motifs in PsiP and PsiL. 21
Figure S4. Peptide mass fingerprinting of laccase 22
Figure S5. Alignments of laccase sequences. 23
Figure S6. Syringaldazine-based assay for biochemical laccase characterization. 24
Figure S7. Determination of absolute oxidase activity. 25
Figure S8. MALDI-MS profile of polymerized psilocin 26
Figure S9. Mass spectrometric analysis of psilocin oxidation by Fe^{III} 27
Figure S10. Color development under different conditions of psilocin oxidation 28
Figure S11. FT-IR spectra of blue oligomeric and polymeric product fractions 30
Figure S12. Time-resolved mass spectrometric analysis of psilocin oxidation 31
Figure S13. Plausible mechanism for formation of psilocin oxidation products. 32
Figure S14. *In situ* ^{1}H NMR spectroscopy of psilocin autoxidation 33
Figure S15. *In situ* inverse gated decoupling ^{13}C-NMR 34

References. 35

Experimental Procedures

Materials

Media components, chemicals, solvents, reagents, and kits were purchased from Promega, Roth, Sigma-Aldrich, and VWR, except psilocybin (**1**) and psilocin (**2**), which were isolated from *Psilocybe cubensis* FSU12409 carpophores. Cultivation, extraction, and extract defatting was done as described.[1] Pre-fractionation was done by preparative HPLC (method P-1, see below).

Instrumentation

NMR spectra were recorded at 300 K on a Bruker Avance III spectrometer at 600 and 150 MHz to record ^{1}H and ^{13}C NMR spectra, respectively. The field strength was 14.09 T; the solvent was MES and BIS-TRIS-buffered D_2O (see section NMR spectroscopy for details). Infrared spectra were recorded on a Jasco FTIR 4100 spectrometer equipped with a diamond ATR sampler (PIKE Technologies MIRacle). Proteins were purified on a GE Healthcare ÄktaPure 25 FPLC System. Mass spectrometry for peptide fingerprinting and high resolution mass spectra was performed on a Dionex Ultimate 3000 UHPLC, connected to a Q Exactive Plus hybrid quadrupole orbitrap mass spectrometer (Thermo Scientific). Analytical HPL chromatography and standard mass spectrometry was done either on an Agilent 1290 Infinity II UPLC instrument or an Agilent Infinity 1260 chromatograph, each coupled to a 6130 quadrupole mass detector. For preparative HPL chromatography an Agilent 1260 preparative chromatograph was used, while semi-preparative applications were run on either an Agilent Infinity 1260 or an Agilent 1200 chromatograph. To record UV/Vis spectra of **2** oxidation products (shown in Figure S10), an Analytik Jena ScanDrop photometer was used. UV/Vis spectra of the compound with *m/z* 405 were extracted from the respective HPLC-detector peak signal (Figure S9).

Production of [$^{13}C_{12}$]psilocin

Aspergillus nidulans tJF03[2] (a genetically engineered high-titer **1** producer) was grown as four 50 mL liquid cultures in *Aspergillus* minimal medium (AMM), supplemented with 3 µl mL^{-1} *p*-aminobenzoic acid (pABA), incubated for 24 h at 37°C and 200 rpm. Cultures were then filtered through Miracloth (Merck), and the biomass was washed with 50 mL of sterile glucose-free AMM and transferred to production medium (AMM with 20 g L^{-1} [$^{13}C_6$]-D-glucose as carbon source, 3 µl mL^{-1} pABA, 50 µg mL^{-1} tetracycline, dispensed into 50 mL Erlenmeyer flasks. Following incubation for 48 h at 30°C at 200 rpm, the biomass was harvested by filtration, shock-frozen in liquid nitrogen, and lyophilized. The broth was acidified with HCl to pH 1.8 and extracted twice with ethyl acetate. The aqueous phase was neutralized with NaOH and lyophilized as well. Dry biomass and broth were extracted with methanol (MeOH) three times. After rotary evaporation, extracts were solved in 0.1% aqueous trifluoroacetic acid (TFA), sonicated, and filtered through cotton wool. [$^{13}C_{12}$]psilocybin was purified chromatographically from these solutions (HPLC methods P-1 and P-2).

The [$^{13}C_{12}$]psilocybin-containing fraction (5.5 mg) was used for enzymatic conversion to [$^{13}C_{12}$]psilocin in 3.9 mL buffer (20 mM MOPS, 150 mM NaCl, 1mM $Na_2S_2O_4$, pH=7.5) within 30 min at RT by 500 U alkaline phosphatase (Boehringer-Mannheim, 500 U $µL^{-1}$). The enzyme was removed by centrifugation in an Amicon filter (Merck, 10 kDa cut off), and the membrane was washed with 0.1% aqueous TFA. Combined filtrates were dried by

lyophilization. [$^{13}C_{12}$]psilocin was purified using preparative HPLC method P-1, yielding 3.27 mg of [$^{13}C_{12}$]psilocin hydrotrifluoroacetate salt.

Purification of psilocin (2)

Purification of **1** was achieved by semipreparative HPLC (method P-2) and subsequent crystallization from cold H_2O. Hydrolysis of **1** to produce **2** was done similar to Hofmann's protocol.[3] Fractions containing **1** from semipreparative HPLC (up to 80 mg) were dissolved in 10 ml H_2O and transferred to a pressure resistant glass tube. A stream of nitrogen was passed into the solution for a few minutes via a stainless steel capillary. The reaction tube was sealed with a steel-capped septum immediately upon stopping the nitrogen flow. Hydrolysis was achieved by heating at 150°C for 1 h. Once finished, solution was frozen and lyophilized. Final purification was done by preparative (method P-1) or semipreparative HPLC (method P-3), depending on amount and nature of impurities. Lyophilization of HPLC fractions yielded hygroscopic psilocin hydrotrifluoroacetate salt, which was used for the majority of experiments due to its polar solubility characteristics. For use as analytical reference compound, however, the salt was dissolved in H_2O with excess $Na_2S_2O_4$, adjusted to pH 10, and extracted with diethyl ether to yield the free psilocin base after solvent removal by rotary evaporation.

Fungal biomass production

Carpophores of *Psilocybe cubensis* FSU12409 were used for purification of native proteins. The fungus was routinely maintained on malt extract peptone (MEP) solid medium (30 g L^{-1} malt extract, 3 g L^{-1} peptone,18 g L^{-1} agar, pH=5.6) at 25°C. To induce carpophore formation, the fungus was grown on a mixture of potting soil/bark humus/perlite. For protein extraction, 10 g (fresh weight) of carpophores were frozen in liquid nitrogen and ground up with mortar and pestle.

Purification of native enzymes from *Psilocybe* carpophores

Native proteins PsiP and PsiL were purified by sequential anion exchange (AIEC), hydrophobic interaction (HIC), and size-exclusion chromatography (SEC). Fractions were screened for enzyme activity by colorimetric assays (below). The powdered biomass was buffered in 50 mL of AIEC buffer A (50 mM NaCl, 25 mM TRIS, pH=7.0). After centrifugation (20,000 × g, 4°C), chromatographic separation was performed on a GE Healthcare ÄktaPure 25 FPLC System equipped with a Q-sepharose Fast Flow column (50 mL bed volume) at a flow of 1 mL min^{-1}. The column was equilibrated in buffer A, and washed for 25 min with buffer A after loading. For elution, a linear gradient 0-100% AIEC buffer B (1.5 M NaCl, 25 mM TRIS, pH=7.0) over 75 min was applied.

HIC was carried out on the same instrument with a HiTrap Phenyl HP column (1 mL bed volume) as stationary phase and at a flow rate of 1 mL min^{-1}. To prepare positive AIEC fractions for HIC, they were re-buffered in HIC buffer A (1.6 M $(NH_4)_2SO_4$, 20 mM MOPS, pH=7.5) using PD-10 columns. After loading the column, it was washed for 5 min with 95% HIC buffer A and 5% HIC buffer B (50 mM $(NH_4)_2SO_4$, 20 mM MOPS, pH=7.5). For elution, a linear gradient 5-100% buffer B over 30 min was applied, followed by an isocratic step (100% B) for 10 min.

For SEC, the above instrument, a Superdex 200 increase 10/300 GL column (24 mL bed volume), and SEC buffer (20 mM MOPS, pH=7.5) were used. HIC protein fractions were re-buffered to SEC buffer and concentrated on Amicon filters (10 kDa cut off) prior to loading. Proteins were eluted in SEC buffer during an isocratic run over

48 min. Fractions were concentrated on Sartorius VivaSpin columns (30 kDa cut-off). SDS-PAGE and silver staining was used to verify purification.

***In vitro* assays for enzymatic activity**

Assays with chromogenic substrates were carried out in 384-well plates (Greiner, flatbottom) using a Clariostar plate reader (BMG Labtech) with automatic substrate injection and appropriate path-length correction. To screen for enzymatically active fractions *in vitro*, chromatographic fractions from AIEC or HIC were used in the respective buffers. Only active fractions were re-buffered to SEC buffer. SEC fractions were assayed without further processing. The activity of aliquots sampled before/during individual FPLC runs were analyzed in parallel, i.e., during the FPLC runtime, in standardized assays (below) to follow enzyme activity over the course of the purification. Leftovers from the samples were frozen at -20°C for later protein quantification and to determine relative specific activities.

a) Detection of phosphatase activity: Phosphatase activity was assayed with **1** and *p*-nitrophenylphosphate (pNPP, 1mM) in 50 µl reactions at 30°C to compare activities of chromatographic fractions or activities in the various buffers. For phosphatase activity on pNPP, the linear slope of the absorption at λ=405 nm was used.

For phosphatase activity on **1** and to determine the pH optimum, phosphatase (in SEC buffer) was tenfold concentrated using 0.5 mL Amicon filter units (10 kDa cut off). The concentrate was diluted 1:10 with Britton-Robinson buffer (H_3PO_4, H_3BO_3, CH_3COOH, each at 40 mM), adjusted to the desired pH with 1 M NaOH. **1** was added to a final concentration of 1 mM. After incubation for 15 min at 30°C, the reactions were stopped by shock freezing in liquid nitrogen, lyophilized, and resuspended in MeOH. After centrifugation at 20,000 × g for 10 min, an aliquot of the supernatant was diluted with nine volumes of 0.1% aqueous formic acid (FA) and analyzed by LC-MS (method A-1).

b) Detection of laccase activity: for specific comparisons of activities or to determine the temperature optimum, the generic laccase substrate syringaldazine (26.1 µM) was used. Reactions were run in SEC buffer and in a total volume of 30 µL and 30°C. To determine the pH optimum, assays were run in Britton-Robinson buffer (20 µL) at the respective pH. For screening of fractions during enzyme purification, any other employed buffer was acceptable. The linear slope of the absorption at λ=530 nm was used to determine enzyme activity. To calculate absolute enzymatic activity (SEC fraction, HIC fraction, *Myceliophthora thermophila* laccase produced in *Aspergillus oryzae*, Sigma SAE0050/Novozyme 51003, *Trametes versicolor* laccase (Sigma-Aldrich 38429), an extinction coefficient of 65 mM^{-1} cm^{-1} was used. The activity was expressed in LAMU (Laccase *Myceliophthora* Units, syringaldazine oxidation in µmol min^{-1} at 30 °C and pH=7.5).[4] Laccase activity on **2** was measured accordingly, using 1 mM substrate in a 50 µL reaction and absorption at λ=618 nm as readout (linear slope).

Mass spectrometry-based peptide fingerprinting and protein identification

Positive SEC fractions were re-buffered in NH_4HCO_3 buffer (50 mM, pH=8.1), digested with 50 µg trypsin per milligram of protein, for 18 h at 37°C. Peptides were extracted using a ZipTip C18 column (Millipore) according to the manufacturer's protocol. The column was washed with solution A (5% acetonitrile (ACN) + 0.1% FA in H_2O) and eluted with solution B (50% ACN + 0.1% FA in H_2O). Ten µL were injected into a Dionex Ultimate 3000 UHPLC, connected to a Q-Exactive Plus hybrid quadrupole orbitrap mass spectrometer, equipped with a heated electrospray ion source. The peptide mixture was separated on a Phenomenex Aeris Peptide XB-C_{18} column

(1.7 µm, 150 × 2.1 mm), coupled to a SecurityGuardTM ULTRA guard cartridge (2 × 2.1 mm) at 40°C and at a flow of 200 µL min^{-1} Mobile phase A was 0.1% FA in water, B was 0.1% FA in ACN. The gradient was: 0-2 min, 1% B; 9 min, 9% B; 38 min, 55% B; 39-44 min, 99% B. Peptides were selected for fragmentation according to their signal intensities, and the top ten signals subjected to data-dependent MS^2-analysis. The precursor scan range was set to *m*/*z* 375-2000, resolving power to 70,000 full width at half maximum (FWHM) at *m*/*z* 200, injection time to 100 ms; and automatic gain control (AGC) to 1×10^6. The data-dependent fragmentation followed with a resolution of 17,500 FWHM at *m*/*z* 200, AGC 1×10^5, maximum injection time of 150 ms, isolation window of *m*/*z* 2.0, normalized collision energy of 30, and dynamic exclusion time of 15 s.

A protein search database was obtained by *in silico* translation of the *Psilocybe cubensis* v1.0 gene catalog of the Joint Genome Institute's MycoCosm.[5] Peptide fragmentation spectra were searched against theoretical mass spectra using MaxQuant.[6] Here, the minimum peptide length considered was seven amino acids, up to three missed tryptic cleavages were accepted. The first round of the peptide search using Andromeda software[7] had a 20 ppm tolerance for the peptide masses, whereas in the main search this parameter was narrowed to 4.5 ppm. False discovery rates were controlled to a maximum of 1% at both peptide match spectrum (PSM) and protein group levels. Moreover, methionine oxidation and *N*-terminal acetylation were allowed as variable modifications. Annotations of identified protein were obtained from the JGI database.

Protein quantification

Protein content of aliquots of crude extracts and AIEC fractions in SEC buffer were determined using Lowry's method,[8] modified for 96-well plates. Solutions were prepared in ddH_2O as follows:

Solution A: Na_2CO_3 20 g L^{-1}, NaK tartrate tetrahydrate 200 mg L^{-1}, NaOH 4 g L^{-1}

Solution B: $CuSO_4$ pentahydrate 5 g L^{-1}

Solution C: Freshly prepared mixture of A and B in a 25:1 ratio

Solution D: Folin-Ciocalteu's phenol reagent (Merck), 1N.

Aliquots (30 µL) of FPLC fractions (diluted when required), were pipetted into a 96-well plate. For reference, 30 µL aliquots of a bovine serum albumine standard series, ranging from 80 to 400 µg mL^{-1}, were used. 200 µL of solution C was added, and the assay was incubated for 15 min at RT. After adding 20 µL of solution D, the plate was shaken for 30 s at 500 rpm and further incubated for 30-120 min. The absorbance was recorded at λ=750 nm using a Clariostar reader (BMG Labtech). Concentrations of HIC and SEC fractions were close to or below the detection limit of colorimetric test. Therefore, quantification was carried out by direct photometric measurement in a 100 µL Hellma quartz microcuvette (1 cm path length). Prior to quantification, samples were desalted using 0.5 mL Amicon filters. Absorbance was photometrically read at λ=228.5 nm and 234.5 nm. The protein amount was calculated with the following formula.[9]

$$\rho = (A_{228.5nm} - A_{234.5nm}) \times 317.5\,\mu g/mL$$

Oxidation of psilocin for LC-MS

a) Iron-mediated oxidation: 50% aqueous MeOH was pre-chilled on ice. Aqueous stock solutions of **2** and $FeCl_3$ were added at final concentrations of 250 µM and 500 µM respectively. The mixture was briefly vortexed

and kept on ice for 20 min. The reaction was stopped by adding EDTA (final concentration 550 µM). The solution was analyzed by LC-MS (method A-2, see below). Additionally, reactions with **2** and $FeCl_3$ (250 µM each, added as aqueous solutions) were set up in H_2O at 5°C and MeOH, pre-chilled to 5 or -18 °C, and kept for 3 d. Mixtures were analyzed directly by LC-MS as described above. Observed relevant mass signals were re-analyzed by high-resolution mass spectrometry and MS/MS (H-1, below).

b) Enzymatic oxidation: 2 (500 µM, in PBS) was oxidized in a glass vial by 0.1 µL mL^{-1} *Myceliophthora thermophila* laccase preparation[10] and with air (40 mL min^{-1}) supplied through a stainless steel capillary. After 3.5 min long aeration intervals, the air supply was interrupted for 1.5 min, and an aliquot of 5 µL was analyzed by mass spectrometry (5 min measurement interval, method A-3, see below). The substrate and products absorbing at λ=600 nm were detected with a peak delay of 0.32 min after injection. Corresponding mass spectral scans were averaged in a 0.2 min time corridor.

c) Autoxidation: solutions of **2** (1 mM) in Britton-Robinson buffers (pH 5, 6, 7, 8, or 9), along with corresponding blanks, were kept in a clear well plate at RT. An additional autoxidation assay for HRMS and MS/MS (method described below) was prepared in unbuffered ddH_2O and treated equally. After 3 d, solutions were directly analyzed by LC-MS (method A-4, see below) and confirmed by HRMS and MS/MS (H-1, below).

UV/Vis spectroscopy during psilocin oxidation

UV/Vis spectra (200-730 nm) were recorded on an Analytik Jena ScanDrop photometer. Samples were blanked to PBS buffered enzyme solutions (enzymatically mediated oxidations) or neat solvent (Fe^{III} mediated oxidations). The **2** concentration was 93 µM (added as 100 mM methanolic stock solution). Used enzymes were laccase from *Myceliophthora thermophila* (1.56 µL commercial solution per 1 mL reaction) or 200 mU horseradish peroxidase (Sigma-Aldrich). Oxygen for enzymatic reactions was provided by pipetting air into the solution between measurements in the case of laccase, or, with peroxidase, by initially adding H_2O_2 (at 187.5 ppm final concentration). Fe^{III} was used at a final concentration of 375 µM. Reactions were run at room temperature.

Analysis of DNA and protein sequences

Amino acid sequences were aligned with Geneious software (version 7.1.9, Biomatters, Ltd.) or ClustalOMEGA.[11] Similar protein sequences were identified using BlastP.[12] Introns and gene models were predicted by Augustus software.[13] Motif searches in amino acid sequences were carried out using SignalP 5.0[14] (to screen for signal peptides), the NetNGlyc 1.0 and NetOGlyc 4.0 servers[15] (for *N*- and *O*-glycosylation sites, respectively, and LocSigDB[16] for protein sorting signals.

Infrared spectroscopy

To record IR spectra, **2** (4 mM, solved in 75% aqueous methanol) was oxidized by $FeCl_3$ at a final concentration of 10 mM. After 4 min at RT, the reaction was briefly chromatographed on a 90 × 10 mm Sephadex LH-20 column with MeOH as mobile phase. To cover oligomers of various sizes, an early- and a late-eluting deep blue fraction were collected, and measured in dried state.

SUPPORTING INFORMATION

Analytical chromatography

Analytical HPLC was performed on an Agilent 1290 Infinity II UPLC instrument with a diode array detector (DAD) and interfaced to a 6130 quadrupole mass detector using ESI (methods A-1, A-3, and A-4) or an Agilent Infinity 1260 chromatograph with diode array detection and a 6130 quadrupole mass detector with an ESI source (method A-2).

Method A-1: a Phenomenex Luna Omega Polar C_{18} 50 × 2.1 mm (1.6 µm particle size) equipped with a guard column was used. The chromatographic separation was accomplished at 30°C and a flow of 0.4 mL min^{-1}, detection was at λ=280 nm. Mobile phase A was 0.1% aqueous FA, phase B was ACN, and a linear gradient was applied (% B) initially 1%, within 2.2 min to 15%, and within further 0.8 min to 100%.

Method A-2: the column was an Zorbax Eclipse XDB-C_{18} 150 × 4.6 mm (5 µm) and a corresponding guard column. Separation was at 25°C and a flow of 1.0 mL min^{-1}, DAD chromatograms were extracted at λ=600 nm, the mass detector was run in positive mode. Mobile phase A was 0.1% aqueous TFA, phase B was ACN. The linear gradient was (% B) initial hold for 3 min at 5%, then within 12 min to 40%, within further 3 min to 100%.

Method A-3: The LC column was replaced by a union as dummy, the 0.3 µm inline filter was kept. The run was carried out at 25°C and a flow of 0.5 mL min^{-1}, DAD chromatograms were extracted at λ=600 nm, the mass detector was run in positive mode. Solvent A was 0.1% aqueous FA, solvent B was ACN. An isocratic flow of 95% A:5% B was applied.

Method A-4: as described for A-1, but at a flow of 0.8 mL min^{-1}, and a modified linear gradient (indicated in % B) of initially 1%, within 2 min to 7%, and within further 8 min to 100%. Detection was at λ=280 nm.

Method H-1 for high-resolution mass spectrometry: High-resolution and MS/MS spectra were recorded on a Thermo Dionex Ultimate 3000 LC system with a C_{18} column (Phenomenex Luna Omega C_{18}, 100 × 2.1 mm, 1.6 µm particle size, 100 Å pore size) coupled to a Thermo Q Exactive Plus spectrometer, using ESI in positive mode (resolving power 70,000 at 200 *m/z*). Solvents were water (A) and ACN (B), both acidified with 0.1 % FA, at a flow rate of 0.4 mL min^{-1}. The linear gradient was from 5% to 10% B in 1 min, from 10% to 90% in 10 min, from 90% to 99% in 1 min, holding for an additional minute. The column was maintained at 40°C.

Preparative chromatography

Method P-1: an Agilent 1260 preparative chromatograph with a Zorbax Eclipse XDB-C_8 column (250 × 21.2 mm, 7 µm) operated at a flow of 20 mL min^{-1} were used. Mobile phase A was 0.1% aqueous TFA, phase B was ACN. The linear gradient was (% B) initial hold for 2 min 10%, within further 3 min to 20%, held at this ratio for further 6 min, then to 100% within 1 min. Chromatograms were recorded at λ=280 nm.

Method P-2: an Agilent Infinity 1260 semipreparative chromatograph with diode array detection, a Thermo Hypercarb column (150 × 10 mm, 5 µm) and a Zorbax Eclipse XDB-C_{18} (15 × 9.4 mm, 5 µm) as guard column were used. Separation took place at 23°C and a flow of 2.5 mL min^{-1}, DAD chromatograms were extracted at λ=600 nm. Solvent A was 0.1% aqueous TFA, solvent B was ACN. A linear gradient (% B) of initially 15%, within 15 min to 36%, and within 1 min to 80%.

Method P-3: an Agilent 1200 chromatograph equipped with a diode array detector and a Zorbax Eclipse XDB-C_8 column (250 × 9.4 mm, 5 µm) was used. Separation was at 25°C and at a flow of 2.5 mL min^{-1}. Solvent A was 0.1% aqueous TFA, solvent B was ACN. The conditions were (% B): initially 5%, within further 2 min to 15%, held at this ratio for further 13 min, then to 100% within 1 min.

SUPPORTING INFORMATION

MALDI mass spectrometry

To record MALDI mass spectra, **2** (8.45 mM) was oxidized with $FeCl_3$ (18.2 mM final concentration) in H_2O. After 3 min at RT, the deep blue solution was loaded onto a Chromabond C18 solid phase extraction cartridge (Macherey-Nagel, 1 g column) and washed three times with H_2O (4 mL each wash). For elution, a step gradient (25, 50, 75, 100% MeOH in H_2O, 4 mL each) was applied. The respective eluted fractions were bulked, and the solvent removed under reduced pressure. The blueish-black residue was re-suspended in 1 mL MeOH. 2 µL suspension were spotted along with 2 µL of the DHAP/DAHC matrix (2,6-dihydroxyacetophenone, 15 mg mL^{-1} in 75% aqueous ethanol with diammonium hydrogen citrate, 10 mM) onto a stainless steel MALDI sample plate. Dried sample was measured on an UltrafleXtreme MALDI TOF/TOF instrument, using a smartbeam-II Laser (Bruker Daltonics, 1000 Hz). Further parameters: reflector mode, positive polarization, mass range *m*/*z* 800-4500 (enabled deflection mode up to *m*/*z* 500), pulsed ion extraction (PIE), 130 ns delay time, manual control mode, 72% laser intensity (laser type 3), and application of 10,000 pulses/250 random pulses in every grid position.

NMR spectroscopy

Enzymatic reaction monitoring ('*in situ* NMR') was done in 5 mm tubes containing sensitivity compatible buffer solutions[17] of MES and BIS-TRIS (100 mM each) in D_2O. **2** was dissolved to give a 5 mg mL^{-1} solution. Before each *in situ* experiment, a blank was recorded with buffer only, followed by a reference spectrum with added substrate. Subsequently, the reaction was initiated by adding 0.525 units horseradish peroxidase (Sigma-Aldrich) and 2.45 µL 30% H_2O_2. Recording of the spectrum began immediately afterward and was repeated periodically (typically in 2-3 min intervals) until signal changes became marginal. Per spectrum, four and 16 scans were recorded in ^1H and inverse-gated decoupling ^{13}C experiments, respectively. In case of autoxidation or pilot measurements with laccase, air was supplied to the NMR tube between spectral recordings by an aquarium pump connected by flexible tubing to a glass capillary that had been produced from a 2.5 mm NMR tube. The capillary was inserted into the measurement tube through a modified 5 mm cap, punctured twice to create a capillary port and an air outlet, respectively. The outlet hole was foam-plugged from the inside to prevent airborne liquid droplets to contaminate the interior of the spectrometer. A fine metering needle valve and a bleeding plug were mounted in-line between pump and capillary, to adjust the air flow into the reaction mixture.

SUPPORTING INFORMATION

Table S1. Peptide mass fingerprinting of the phosphatase-containing protein fraction. The active fraction obtained after size-exclusion chromatography was digested using trypsin and the resulting peptides were analyzed by LC-MS/MS. Tandem-mass spectra of peptides were searched against a protein library deduced from the *Psilocybe cubensis* genome v1.0 (JGI MycoCosm database) using MaxQuant. Selected output of the MaxQuant protein table is shown for each protein identified (JGI accession numbers). Proteins with Andromeda identification scores < 20 were disconsidered for this table. Protein annotations were obtained from the JGI MycoCosm database. The two putative phosphatases are highlighted in yellow.

Majority protein IDs	JGI annotations	Unique peptides	Unique sequence coverage [%]	Mol. weight [kDa]	Sequence length	Score	Intensity	MS/MS count
jgi|Psicub1_1|89927|fgenesh1_pm.NODE_5188_#_2	KOG1382 Multiple inositol polyphosphate phosphatase EC:3.1.3.83 -phytase PF00328 Histidine phosphatase superfamily (branch 2) IPR000560 His_Pase_clade-2 IPR029033 His_PPase_superfam	9.00	20.50	59.42	552.00	323.31	2.13E+08	25.00
jgi|Psicub1_1|90093|fgenesh1_pm.NODE_5257_#_12	KOG0602 Neutral trehalase EC:3.2.1.28 alpha,alpha-trehalase PF01204 Trehalase IPR001661 Glyco_hydro_37 IPR0089286 hairpin_glycosidase_sf	4.00	9.40	67.63	625.00	107.74	6.15E+06	4.00

jgi|Psicub1_1|52035|e_gw1.9136.47.1	KOG2419 Phosphatidylserine decarboxylase EC:4.1.1.65 phosphatidylserine decarboxylase PF12588 Phophatidylserine decarboxylase PF02666 Phosphatidylserine decarboxylase IPR022237 PsiD-like IPR003817 PS_Decarbxylase	4.00	14.10	49.52	441.00	66.72	3.41E+06	4.00
jgi|Psicub1_1|92779|fgenesh1_pm.NODE_7021_#_39	KOG2366 Alpha-D-galactosidase (melibiase) EC:3.2.1.22 alpha-galactosidase PF02065 Melibiase IPR000111 Glyco_hydro_27/36_CS IPR017853 Glycoside_hydrolase_SF	2.00	7.00	51.88	456.00	50.85	1.58E+06	2.00
jgi|Psicub1_1|74822|gm1.3683_g	KOG1382 Multiple inositol polyphosphate phosphatase EC:3.1.3.83 phytase PF00328 Histidine phosphatase superfamily (branch 2) IPR000560 His_Pase_clade-2 IPR029033 His_PPase_superfam	2.00	4.10	72.38	653.00	24.36	1.48E+06	2.00
CON__P07477		1.00	4.00	26.56	247.00	20.41	7.74E+06	3.00

Table S2. Characteristics of biosynthetic genes *psiP* and *psiL* in *P. cubensis*.

gene	GenBank accession number	length including introns (bp)	number of introns	cDNA length	verified function of gene product	Position in *P. cubensis* genome
psiL	MN117956	2333	13	1587	psilocin laccase	NODE_268:6176-16492
psiP	MN117957	2138	9	1659	psilocybin phosphatase	NODE_5188:21281-23415

SUPPORTING INFORMATION

Table S3. Predicted subcellular localization of PsiP and PsiL. Note that the indifferent localization pattern of PsiL suggests an extracellular localization.

protein	signal	coordinate(s)	localization
PsiP	Yx_2[VILFWCM]	14-18 209-213 251-255 270-274 333-337	Lysosome
	Kx_3Q	513-518	Lysosome
	GYx_2[VILFWCM]	332-337	Lysosome
	[HK]xK	547-550	Endoplasmic reticulum
PsiL	[DE]x_3L[LI]	189-195	Lysosome/melanosome
	Yx_2[VILFWCM]	16-20 156-160 270-274	Lysosome
	SPS	363-366	Nucleus
	DxE	163-166	Endoplasmic reticulum
	[HK]xK	92-95	Endoplasmic reticulum

Table S4. PsiP-like enzymes in psilocybin-producing mushrooms and *Coprinopsis cinerea*. No PsiP homologs could be identified in *Stropharia aeruginosa*. *Translational start and stop codons in *Panaeolus cyanescens psiP* (CVT24_006084) are incorrectly annotated. Comparative sequence analysis and protein alignment with *P. cubensis* PsiP revealed an expected protein size of 553 aa.

organism	locus/protein ID	e value	protein identity	length (aa)	JGI or NCBI accession number
Psilocybe cubensis	Psicub1_1|89927	0	100.00%	552	fgenesh1_pm.NODE_5188_#_2
Psilocybe cyanescens	CVT25_006297	0	86.03%	549	PPQ83612.1
Psilocybe serbica	Psiser1|41327	0	82.75%	548	e_gw1.182.2103.1
Panaeolus cyanescens	CVT24_006084* CVT24_006084 (corrected)	0 0	64.99% 65.40%	751* 553	PPQ62978.1
Gymnopilus dilepis	CVT26_002688	0	69.48%	554	PPQ64744.1
Coprinopsis cinerea	CC1G_03021	1 x10^{-148}	45.93%	637	XP_001835933.1

.

SUPPORTING INFORMATION

Table S5. Peptide mass fingerprinting of the oxidase-containing protein fraction. The active fraction obtained after size-exclusion chromatography was digested using trypsin and the resulting peptides were analyzed by LC-MS/MS. Tandem-mass spectra of peptides were searched against a protein library deduced from the *Psilocybe cubensis* genome v1.0 (JGI MycoCosm database) using MaxQuant. Selected output of the MaxQuant protein table is shown for each protein identified (JGI accession numbers). Proteins with Andromeda identification scores < 20 were disconsidered for this table Protein annotations were obtained from the JGI MycoCosm database. The putative laccase is highlighted in yellow.

Majority protein IDs	JGI annotations	Unique peptides	Unique sequence coverage [%]	Mol. weight [kDa]	Sequence length	Score	Intensity	MS/MS count
jgi|Psicub1_1|33782|e_gw1.1868.111.1	EC:3.2.1.58 glucan 1,3-beta-glucosidase PF12708 Pectate lyase superfamily protein IPR011050 Pectin_lyase_fold/ virulence	20	48	82.694	781	230.96	8.40E+07	50
jgi|Psicub1_1|71514|gm1.375_g	KOG1263 Multicopper oxidases EC:1.10.3.3 L-ascorbate oxidase PF00394 Multicopper oxidase PF07732 Multicopper oxidase PF07731 Multicopper oxidase IPR011706 Cu-oxidase_2 IPR002355 Cu_oxidase_Cu_BS IPR001117 Cu-oxidase IPR008972 Cupredoxin IPR011707 Cu-oxidase_3	10	24.8	57.444	528	90.369	8.40E+07	26
jgi|Psicub1_1|51021|e_gw1.7121.28.1	KOG2263 Methionine synthase II (cobalamin-independent) EC:2.1.1.145-methyltetrahydropteroyltriglutamate---homocysteine S-methyltransferase PF08267 Cobalamin-independent synthase, N-terminal domain PF01717 Cobalamin-independent synthase, Catalytic domain IPR013215 Cbl-indep_Met_Synth_N	13	26	84.433	765	140.34	8.40E+07	19

	IPR002629 Met_Synth_C/arc IPR006276 Cobalamin-indep_Met_synthase							
jgi|Psicub1_1|71069|fgenesh1_pg.NODE_9212_#_22	EC:4.4.1.5 lactoylglutathione lyase PF12681 Glyoxalase-like domain IPR029068 Glyas_Bleomycin-R_OHBP_Dase IPR025870 Glyoxalase-like_dom	7	81.4	14.053	129	104.68	8.40E+07	9
jgi|Psicub1_1|90109|fgenesh1_pm.NODE_5257_#_28	KOG3275 Zinc-binding protein of the histidine triad (HIT) family EC:3.6.1.17 bis(5'-nucleosyl)-tetraphosphatase (asymmetrical) PF01230 HIT domain IPR001310 Histidine_triad_HIT IPR019808 Histidine_triad_CS IPR011146 HIT-like	8	42.7	15.714	143	75.398	8.40E+07	12
jgi|Psicub1_1|71039|fgenesh1_pg.NODE_9136_#_24	None	3	28.6	20.476	185	31.634	8.40E+07	3
jgi|Psicub1_1|93108|fgenesh1_pm.NODE_7170_#_1	EC:3.1.3.2 acid phosphatase PF00328 Histidine phosphatase superfamily (branch 2) IPR000560 His_Pase_clade-2 IPR029033 His_PPase_superfam	3	11.6	50.284	450	21.108	8.40E+07	3

Table S6. PsiL-like enzymes in psilocybin-producing mushrooms and other basidiomycetes.

organism	locus/protein ID	e value	protein identity	length (aa)	JGI or NCBI accession number
Psilocybe cubensis	Psicub1_1|71514	0	100.00%	528	gm1.375_g
Psilocybe cyanescens	CVT25_009559	0	70.40%	522	PPQ94704.1
Psilocybe serbica	Psiser1|66677	0	69.85%	520	e_gw1.42.198.1
Panaeolus cyanescens	CVT24_009838	0	60.82%	524	PPQ71157.1
Gymnopilus dilepis	CVT26_003063	0	62.62%	519	PPQ98001.1
Coprinopsis cinerea	laccase 2 precursor, Lac2	0	62.21%	517	AAD30965.1
Stropharia aeruginosa	yellow laccase, LacY	0	63.19%	518	AFE48786.2

Table S7. Comparison of laccase activity, determined as the amount of enzyme that oxidizes 1 µmol of syringaldazine per minute and mg protein at 30°C and pH 7.5.

enzyme	found activity
PsiL (HIC fraction)	1.1
PsiL (SEC fraction)	0.6
Myceliophthora thermophila laccase	9.3
Trametes laccase	1.2×10^{-3}

SUPPORTING INFORMATION

Table S8. Psilocyl oligomers observed by mass spectrometry. For structures, see Figure S13. †denotes non-ionized compound; ‡ the "+" symbol denotes detected signature fragment ions of the dimethylaminoethyl sidechain (*m*/*z* 58 and *m*/*z* $[M+H]^+$ -45) detected, n.r. data not recorded; *R: direct radical coupling (Figure S13, II), R+N: nucleophilic addition on previous radical coupling products (Figure S13, IV), N: nucleophilic coupling (Figure S13, V). Mass errors between theoretical and observed *m*/*z* values were < 3 ppm; ** if isomeric peaks were detected, retention times are indicated in the order of intensity. Mass spectra were recorded on a Thermo Thermo Q Exactive Plus spectrometer, using ESI in positive mode (see Experimental Procedures, LC-MS Method H-1).

ion	annotation	*m*/*z* $[M+H]^+$ found HRMS	sum formula†	side chain MS/MS‡	formal derivation	plausible mechanism*	t_R.**/min	primarily observed with
205	psilocin (**2**)	205.13358	$C_{12}H_{16}ON_2$	+	P		2.78	
219	quinoid psilocin (**16**)	219.11290	$C_{12}H_{14}O_2N_2$	+	P+[O]-2[H]	N	3.53/2.81	Autoxidation
221	hydroquinoid psilocin (**15**)	221.12845	$C_{12}H_{16}O_2N_2$	n.r.	P+[O]	N	2.35/3.26	Autoxidation
405	quinoid dimer (**6**)	405.22824	$C_{24}H_{28}O_2N_4$	+	2P-4[H]	R	3.57	Enzymatic or Fe(III) oxidation
407	hydroquinoid dimer (**5**)	407.24387	$C_{24}H_{30}O_2N_4$	+	2P-2[H]	R	3.38	Enzymatic or Fe(III) oxidation, Autoxidation at higher concentrations
419	oxoquinoid dimer (**19**)	419.20761	$C_{24}H_{26}O_3N_4$	+	2P+[O]-6[H]	N or R+N	3.89	Autoxidation at lower concentrations
421	hydroxyquinoid dimer (**18a,b**)	421.22372	$C_{24}H_{28}O_3N_4$	n.r.	2P+[O]-4[H]	N or R+N	3.28	Enzymatic or Fe(III) oxidation, autoxidation
423	hydroxyhydroquinoid dimer (**17a,b**)	423.23969	$C_{24}H_{30}O_3N_4$	n.r.	2P+[O]-2[H]	N or R+N	2.08/2.98	Enzymatic or Fe(III) oxidation, autoxidation
435	methoxyquinoid dimer (**24**)	435.23993	$C_{25}H_{30}O_3N_4$	n.r.	2P+[MeOH]-6[H]	R+N	3.67/4.13	Fe(III) oxidation (methanolic)
437	methoxyhydroquinoid dimer (**23**)	437.25507	$C_{25}H_{32}O_3N_4$	n.r.	2P+[MeOH]-4[H]	R+N	3.32	Fe(III) oxidation (methanolic)
449	dioxoquinoid dimer (**20**)	449.18094	$C_{24}H_{24}O_5N_4$	+	2P+2[O]-8[H]	N or R+N	4.19	Autoxidation at lower concentrations
605	quinoid (indolone) trimer	605.32355	$C_{36}H_{40}O_3N_6$	n.r.	3P-8[H]	R	4.28	Enzymatic or Fe(III) oxidation
607	quinoid (indolol) trimer (**8**)	607.33905	$C_{36}H_{42}O_3N_6$	+	3P-6[H]	R	4.09/3.71/3.97	Enzymatic or Fe(III) oxidation
609	hydroquionoid trimer (**7**)	609.35419	$C_{36}H_{44}O_3N_6$	n.r.	3P-4[H]	R	3.80/3.62/3.41	Enzymatic or Fe(III) oxidation, Autoxidation at higher concentrations
621	oxoquinoid trimer (**21**)	621.31845	$C_{36}H_{40}O_4N_6$	+	3P+[O]-8[H]	N or R+N	3.15/3.04/2.94	Enzymatic or Fe(III) oxidation, autoxidation
623	oxohydroquinoid trimer (**22**)	623.33392	$C_{36}H_{42}O_4N_6$	n.r.	3P+[O]-6[H]	N or R+N	2.66/2.60	Enzymatic or Fe(III) oxidation, autoxidation

807	fully quinoid tetramer (**11**)	807.43365	$C_{48}H_{54}O_4N_8$	+	4P-10[H]	R	3.87/3.69/4.06	Enzymatic or Fe(III) oxidation
809	hybrid tetramer (**10**)	809.44922	$C_{48}H_{56}O_4N_8$	n.r.	4P-8[H]	R	3.93/4.03/3.83	Enzymatic or Fe(III) oxidation, Autoxidation at higher concentrations
811	hydroquinoid tetramer (**9**)	811.46509	$C_{48}H_{58}O_4N_8$	n.r.	4P-6[H]	R	3.67/3.53/3.38	Enzymatic or Fe(III) oxidation, Autoxidation at higher concentrations

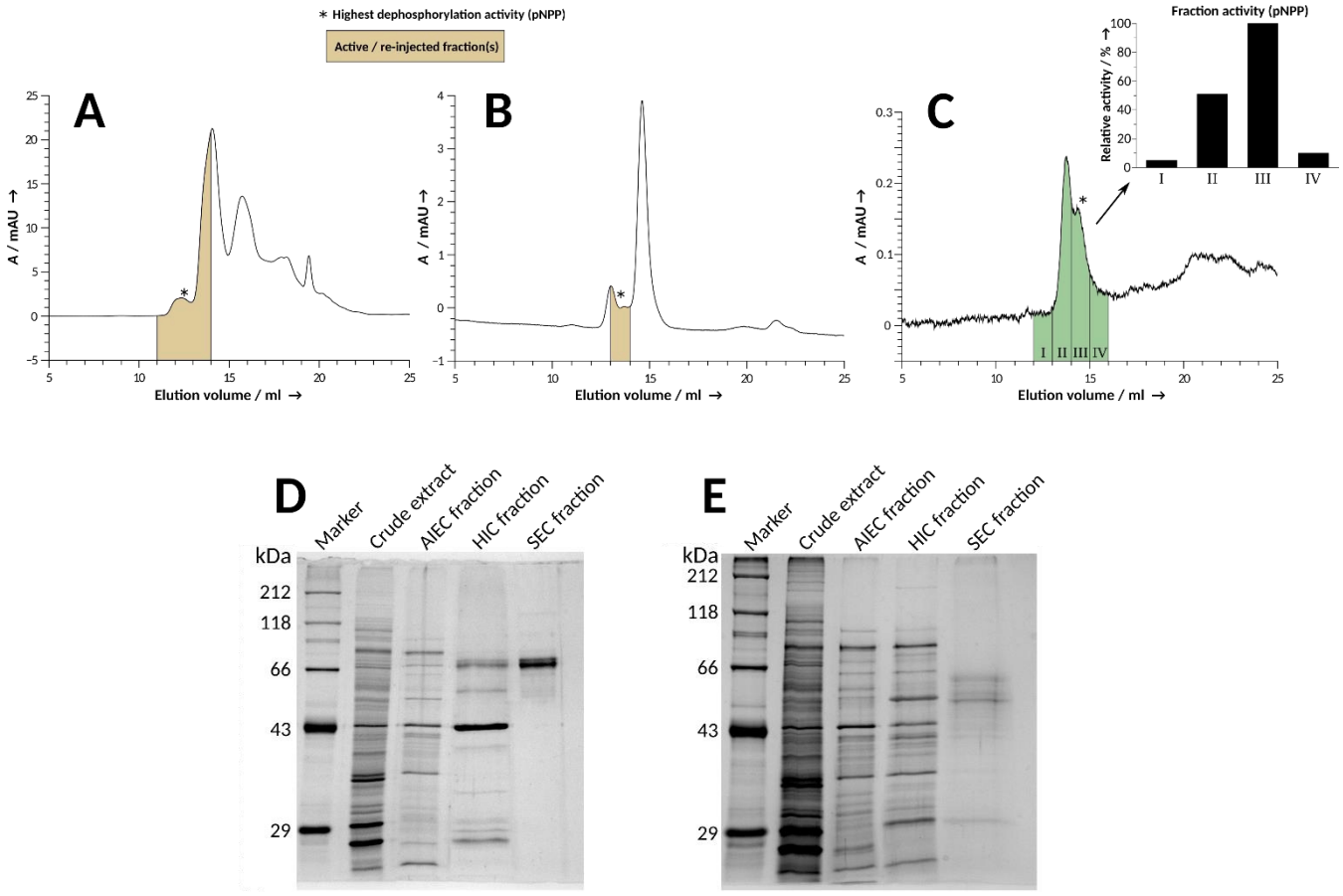

Figure S1. Representative size exclusion chromatograms of the FPLC purification cascades. A) Elution profile of the pre-purified PsiP fraction derived from ion exchange and hydrophobic interaction runs. B) Elution profile of the reinjected fraction highlighted in panel A. C) Elution profile and corresponding phosphatase activity assays of reinjected fraction highlighted in panel B. D) Silver stained polyacrylamide gel to verify PsiP purification. E) Silver stained polyacrylamide gel of PsiL purification. The respective SEC fractions were subjected to protein fingerprinting (Tables S1 and S5).

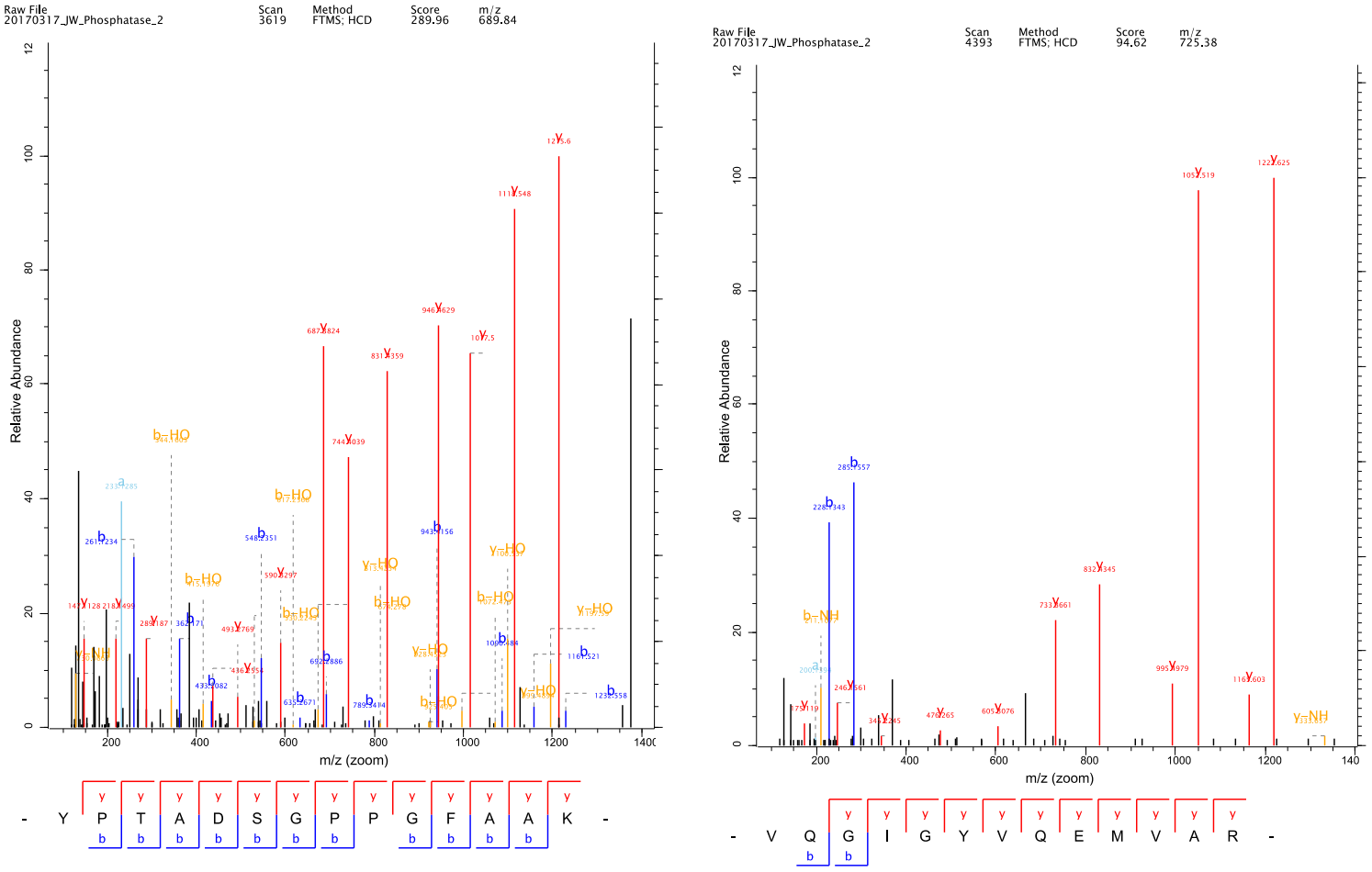

Figure S2. Peptide mass fingerprinting of phosphatases (left:JGI ProteinID 89927; right: 74822). Representative MS/MS spectra of PsiP fragments released by tryptic digest (primary amino acid sequence: 'YPTADSGPPGFAAK' and 'VQGIGYVQEMVAR') are shown. Peaks corresponding to characteristic fragmentation products (e.g. a-, b-, x-, and y-ions) are annotated accordingly. A schematic overview of fragmentation products is shown below the mass spectrum.

PsiP

MHSLGLFALISLLPYLVVAQRASTFAGATTTAVFPPPNAGIAATDTNFPDGSKVGFPGPTRTGDEAAAIETAPVAAKVDS 80
FFPLINGGAEDSTPMDPFDVLVHLGNLSPFQSVPSSAFGLPGASPLIPEGCDIVQAHLLHRHGARYPTADSGPPGFAAKV 160
NAAANSGSGFSAKGDLSFLNTWTYKLGGDILTPFGRSQLFNLGVGFRVKYGQLLKGFKNLPVFRTTSEARMLDSALHFAT 240
GFFGVQKYQDSYHQLITIEHGGKQNNTLAPYESCTNGLNAVAAFGDIQSQKWAQIYLAPAVKRLNANLRGLQLNVTDLFA 320
MQQLCAFETVALGYSSFCDLFTEEEWRGFEYQSDLQFWYSFGPGNPASSAMGIGYVQELVSRLTKTRITTFDTTVNASIV 400
TSDILFPLDQPIYVDATHDTILTAIFAAMNLTTLAANGPLPTDHIPKGQTFFANQLAPFAANVVGQVLSCPASSKPTHIR 480
WIINDGVVPLTGIKGCKPDKNGMCEINTFIAGMKQRMQEIDFNFDCFANYTVPVPDNIVNGQYPQNLKPKKK

PsiL

MNFLLSIATLGLGLQAYAVMIGPSATLVIGNKNIAPDGIKRSAVLAGTSLDTLSFPGPVIRATKGDTLSLNVVNQLTDAT 80
MLMGTSIHWHGFHQKGTSWADGVVGVTQCPIAPGHSFLYQFPTANQAGTFWYHSHYSTQYCDGLRGALIVYDPTDPYRTW 160
YDIDDESTIITLADWYHKAAPLQTLRTAKEDSVLINGQGRVPGDKTTDSTPLSVINIIPQKRYRFRLISISCDPAFSFSI 240
DGHSMTVIEADSQSVQPLTVNEITIFAGQRYSFILYANNPVGNYWIRSQPTYPDDGIQGYAGGINSAILRYSGAPAVNPT 320
TKKASITIPLVEADLRPLYSPAAPGLPSPGAADVNIKLDISYNSPSETFFVNNSTFPEVPVPVLLQILSGAQSANDLLPA 400
GSVYTLPPNKVIEISMPGGRPGSPHPMHLHGHDFSVVRSAGSNRYNYANPVRRDVVNIGMEDTDNVTIRFKTDNSGPWIL 480
HCHIDWHIEAGLAVVFTEDIPSIQFSNPPPAWDQLCPIFNAIPPQKFH

Figure S3. Signal motifs in PsiP and PsiL. Signal peptides were predicted with SignalP 5.0[14] and are highlighted in green. Asn-Xaa-Ser/Thr sequons in the sequences are highlighted in blue in which asparagine residues predicted by NetNGlyc 1.0[15] to be *N*-glycosylated are highlighted in red. Potential *O*-glycosylated Ser/Thr residues are shown in orange and were revealed using NetOGlyc 4.0.[15] For PsiP, an *N*-terminal signal peptide of 19 aa, 17 *O*-glycosylation sites and four *N*-glycosylation sites are predicted. Accordingly, the same software predicted an *N*-terminal signal peptide of 18 aa, three *N*-glycosylation, and seven *O*-glycosylation sites for PsiL. The *O*-glycosylation site at position 320 overlaps with an *N*-glycosylation sequon and is thus shown in blue. In contrast to PsiL, PsiP is likely localized in the lysosomes, as supported by seven potential lysosomal signal peptides, bioinformatically recognized by LocSigDB.[16] See also Table S3.

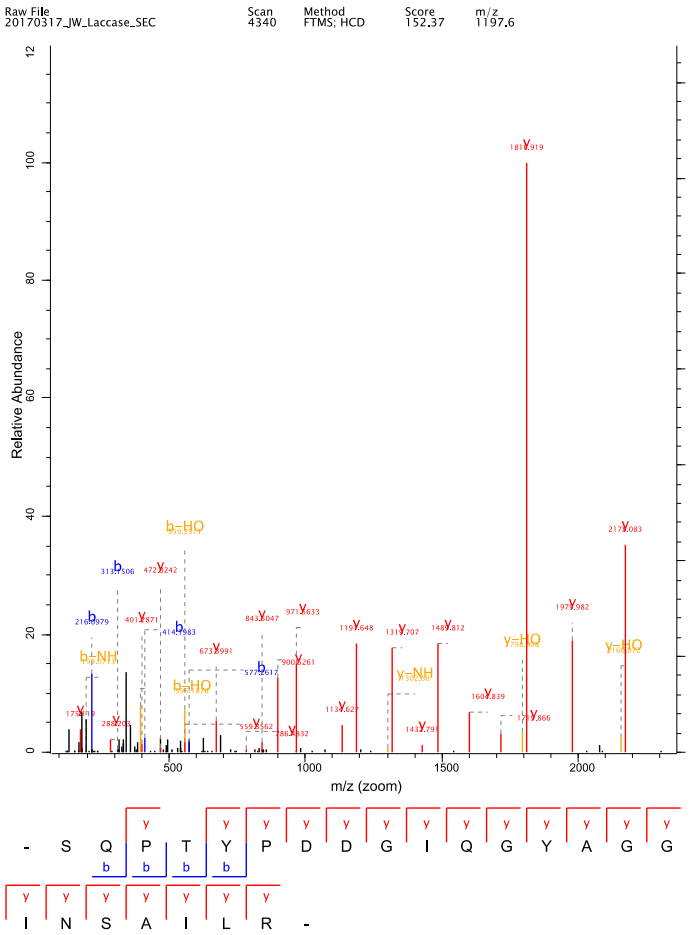

Figure S4. Peptide mass fingerprinting of PsiL (JGI ProteinID 71514). A representative MS/MS spectrum of a PsiL fragment released by tryptic digest (primary amino acid sequence: 'SQPTYPDDGIQGYAGGINSAILR') is shown in the top panel. Peaks corresponding to characteristic fragmentation products (e.g. a-, b-, x-, and y-ions) are annotated accordingly. A schematic overview of fragmentation products is shown below the mass spectrum.

SUPPORTING INFORMATION

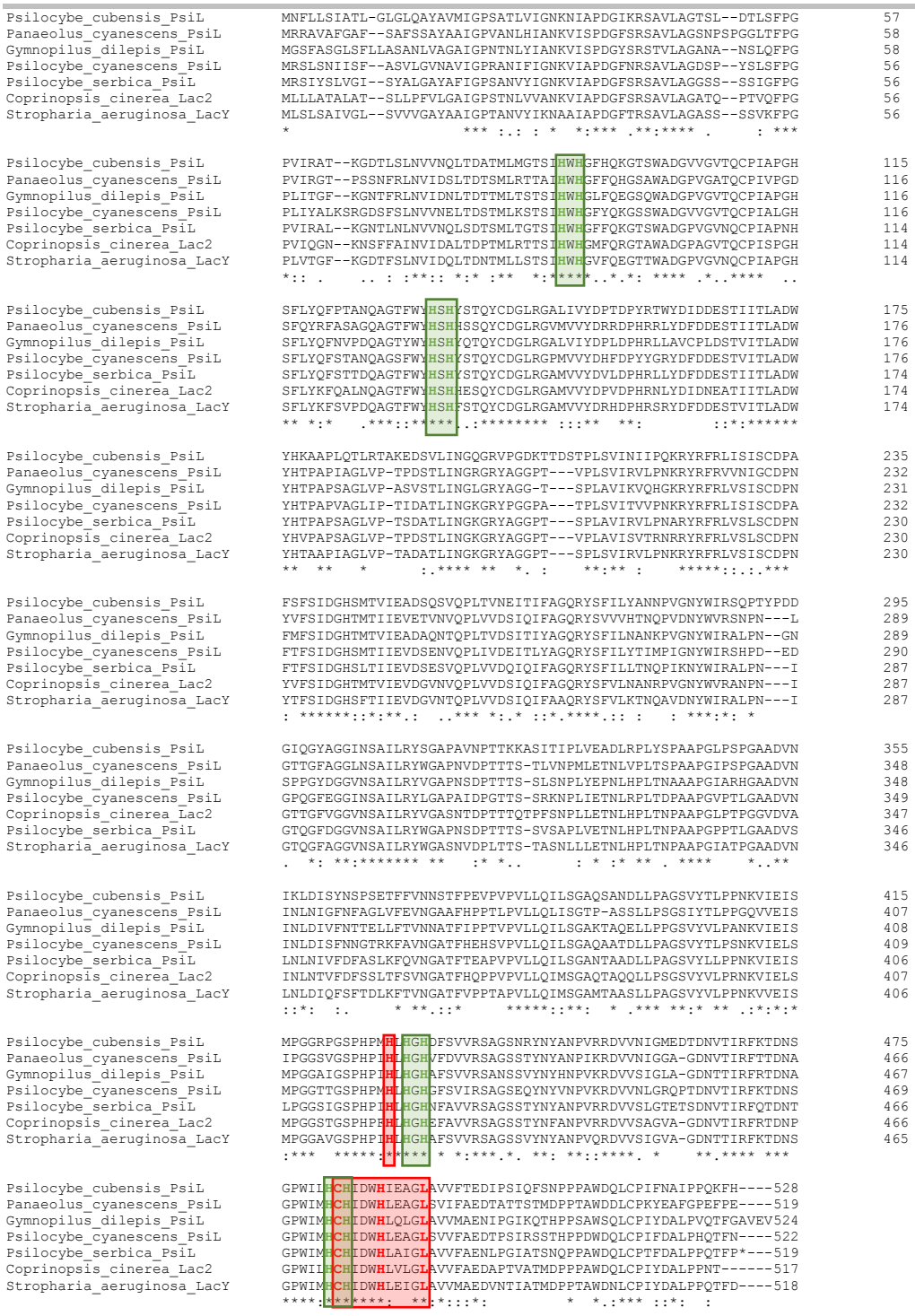

Figure S5. Alignments of laccases, based on the ClustalOmega algorithm,[11] including PsiL from *P. cubensis*, putative laccases from other psilocybin producers, yellow laccase (LacY) from *S. aeruginosa*, and laccase 2 (Lac2) from *C. cinerea*. Shared amino acid residues in the copper ion coordination sites type 1 and type2/type3 are highlighted in green and red, respectively. PsiL shows a typical mononuclear type 1 Cu coordination site (His425, Cys482, His487) with an adjacent conserved leucine residue (Leu492). Cu ions in the trinuclear type2/type3 site are presumably coordinated by His residue pairs 88/90, 133/135, 428/430, and 481/483.

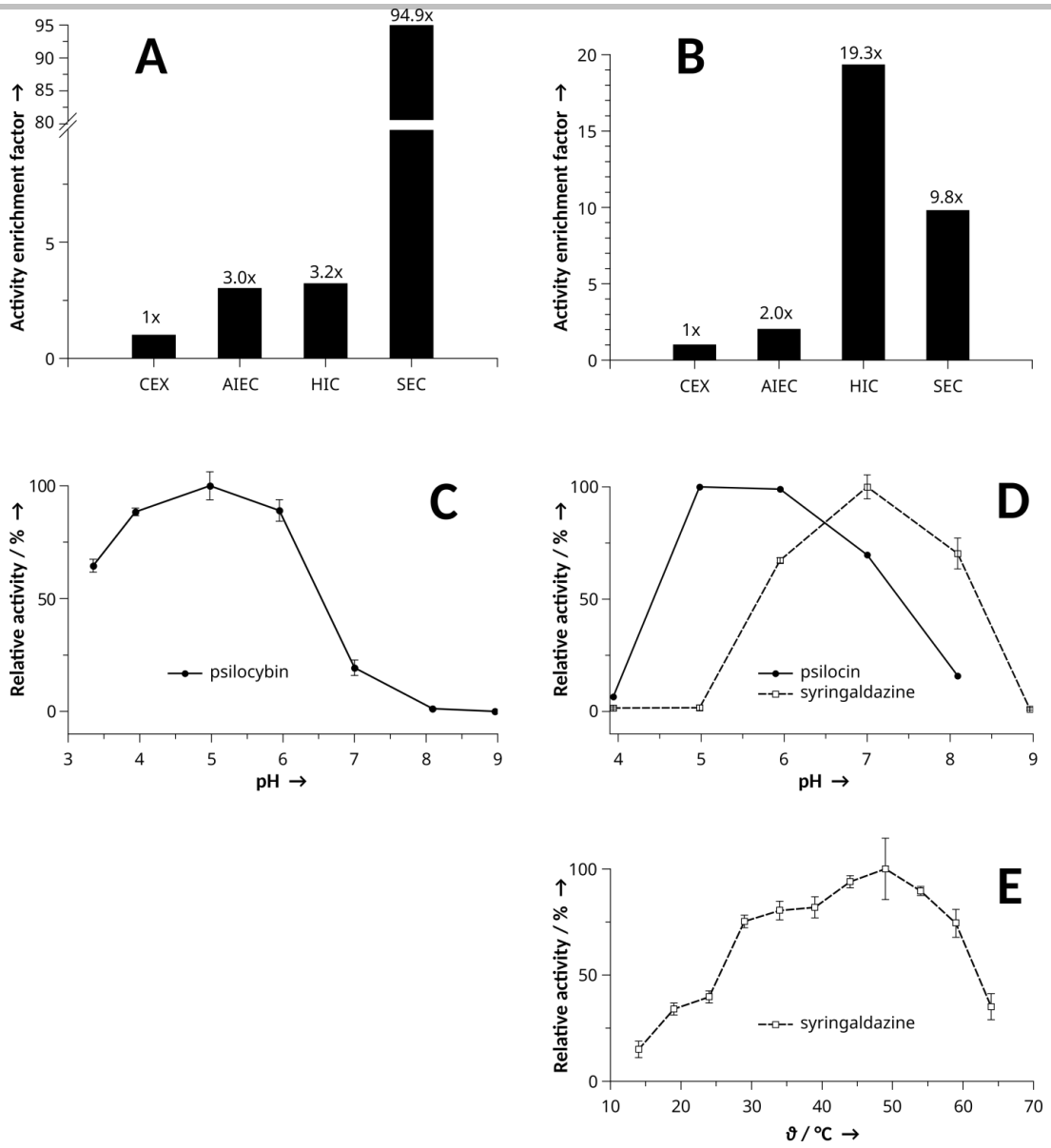

Figure S6. Enzyme characterization of PsiP and PsiL. CEX - crude extract, AIEC - fraction after anion exchange chromatogrphy purification, HIC – fraction after hydrophobic interaction chromatography purification, SEC – fraction after size exclusion chromatography purification. A) Enrichment of specific phosphatase activity during PsiP purification cascade based on 4-nitrophenyl dihydrogen phosphate (pNPP) dephosphorylation assays. B) Enrichment of specific oxidase activity during the PsiL purification steps based on syringaldazine oxidation assays. C) Determination of the pH optimum of **1** dephosphorylation by PsiP. Optimum turnover occurred at pH 5, which is consistent with other fungal acid phosphatases[18] and compatible with its likely storage in acidic compartments. D) Determination of the pH optimum of **2** and syringaldazine oxidation by PsiL. The pH optimum was at pH 7 with syringaldazine and in a plateau between pH 5 and 6 for **2**. Optimum turnover was at 50 °C. E) Determination of the temperature optimum, determined by PsiL-catalyzed syringaldazine oxidation.

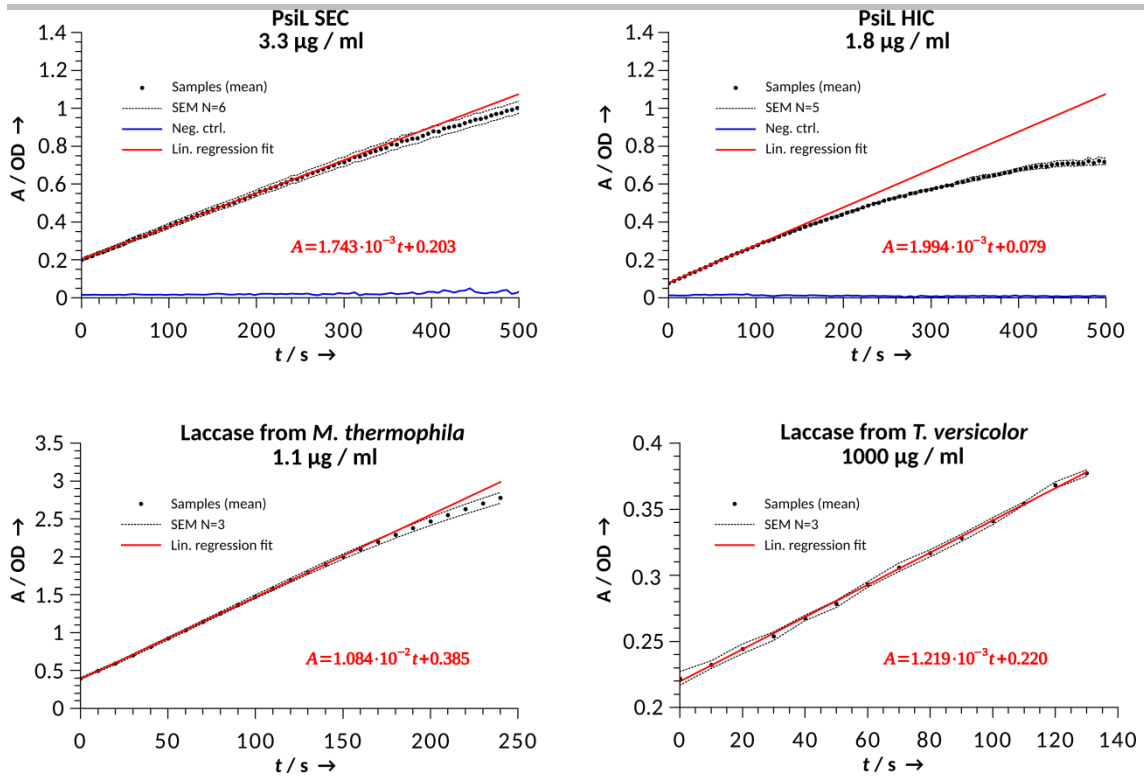

Figure S7. Determination of absolute oxidase activity of selected laccases using syringaldazine as a chromogenic substrate. SEM – standard error of the mean, N – number of replicates. See also Table S7.

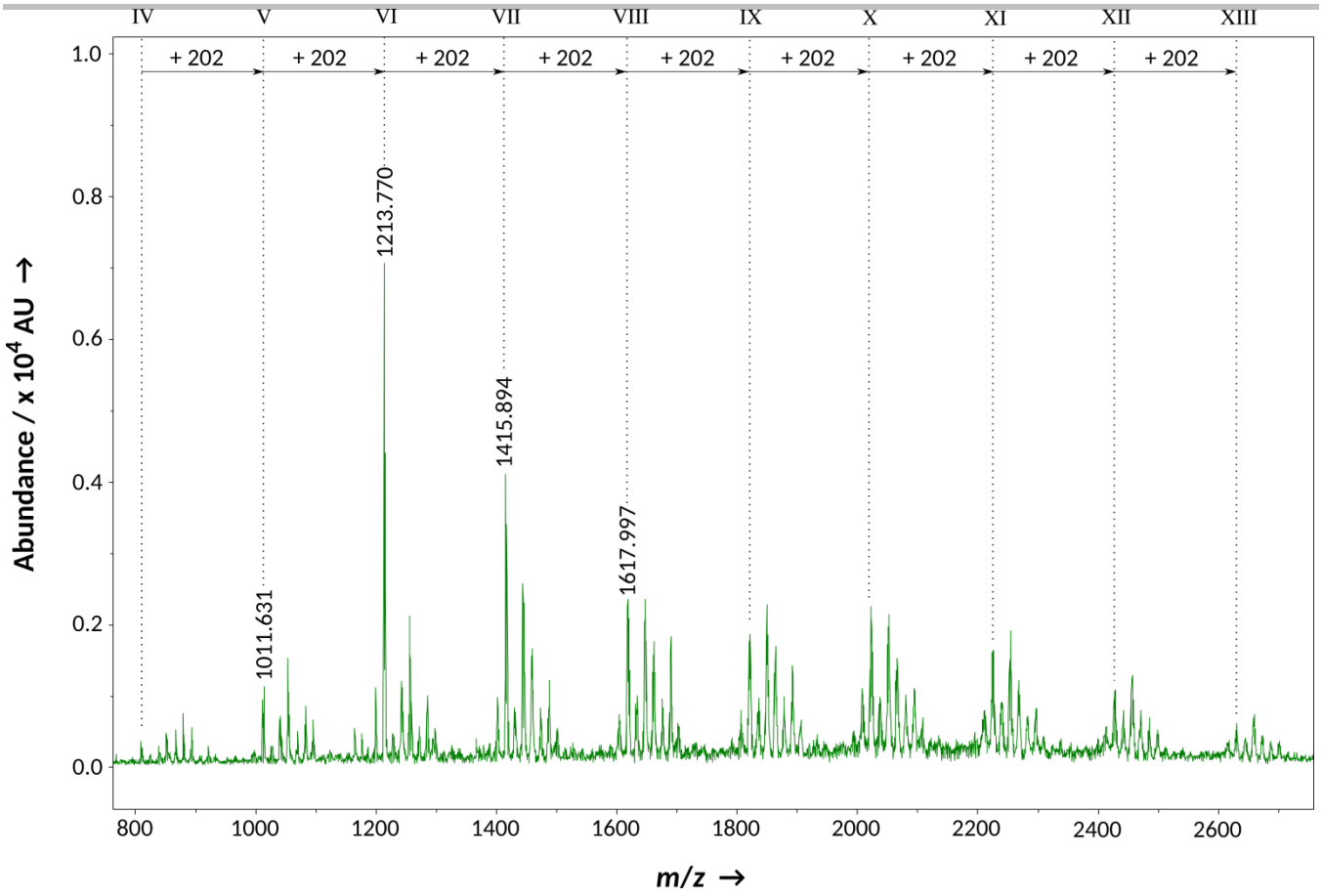

Figure S8. MALDI-MS profile of polymerized **2** with a degree of polymerization of 4 to 13. The difference of *m*/*z* 202 between the adjacent oligomers corresponds to [psilocin-2H].

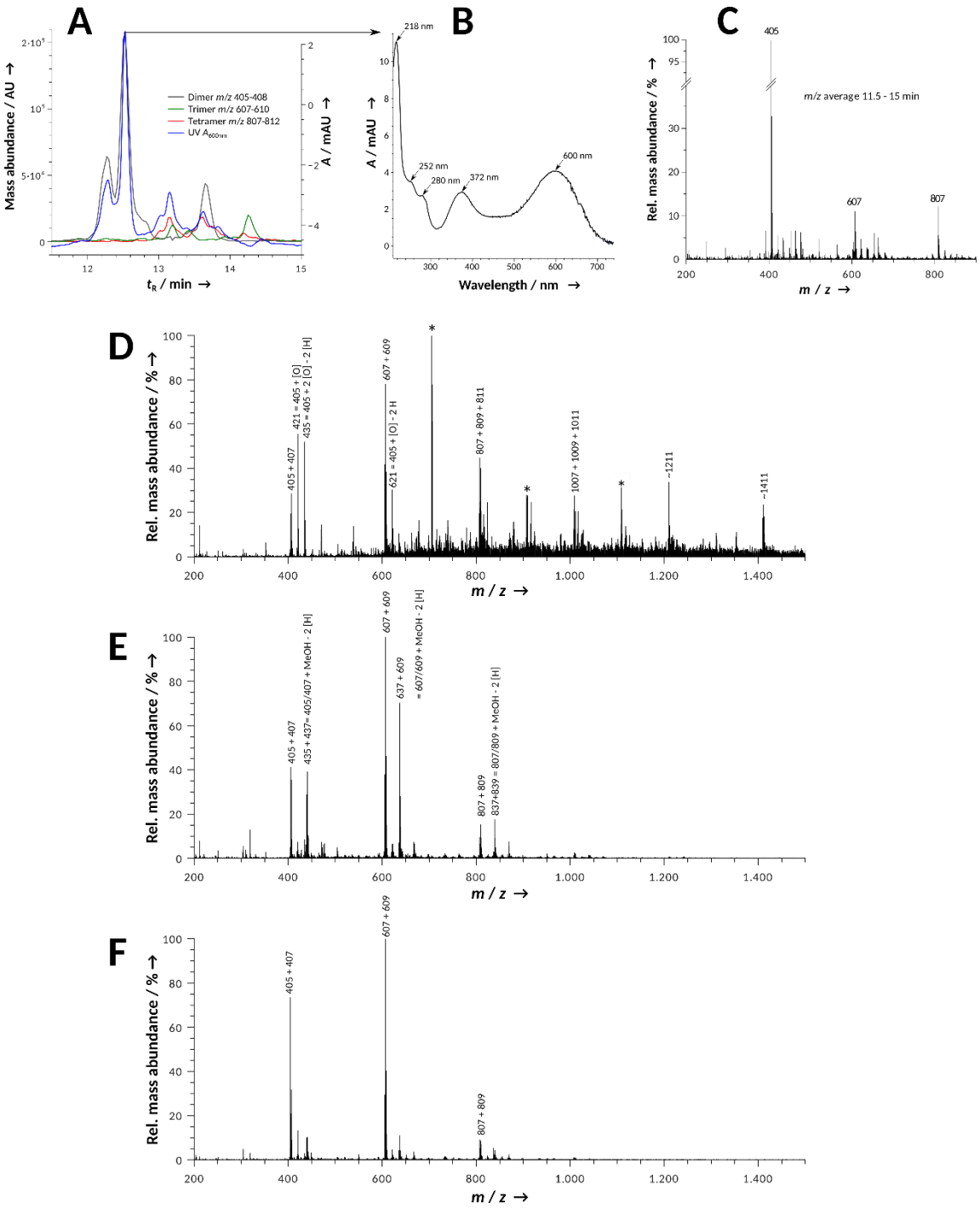

Figure S9. LC-MS analysis of **2** oxidation by Fe^{III}. A) Reaction of 250 µM **2** and 500 µM $FeCl_3$ for 20 min on ice. Overlay of EICs of oligomeric products with the UV/Vis signal at λ=600 nm to detect blue color. The highest ratio of absorption to mass abundance was observed with dimer 405 at t_R=12.5 min (putatively one blue chromophore) and tetramer 807 at t_R=13.15 min (putatively two blue chromophores). Isomeric forms occasionally show less or no absorption at λ=600 nm. B) UV/Vis spectrum extracted at the apex (arrow) of the signal at t_R=12.5. C) Averaged mass spectra over the time range of eluting colored products for the identical reaction. D) Reaction of **2** and $FeCl_3$ (250 µM each) in H_2O at 5 °C for 3 d, that yielded a **2** turnover of ~89%. Asterisks indicate doubly charged $[M+2H]^{2+}$. E) **2** and $FeCl_3$ (250 µM each) in methanol at 5 °C for 3 d. The **2** turnover was ~67%. F) **2** and $FeCl_3$ (250 µM each) in methanol at -18 °C for 3 d, which led to a **2** turnover of ~53%.

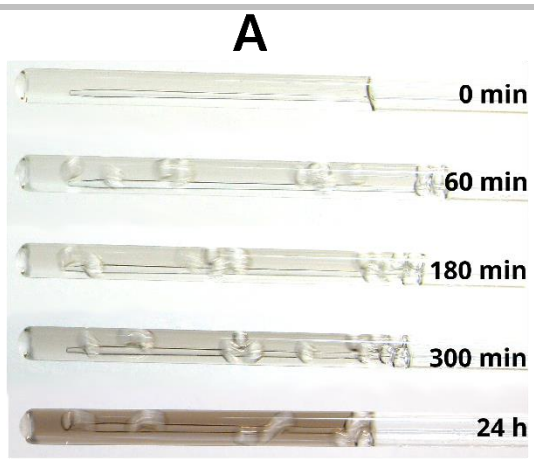
A
0 min
60 min
180 min
300 min
24 h

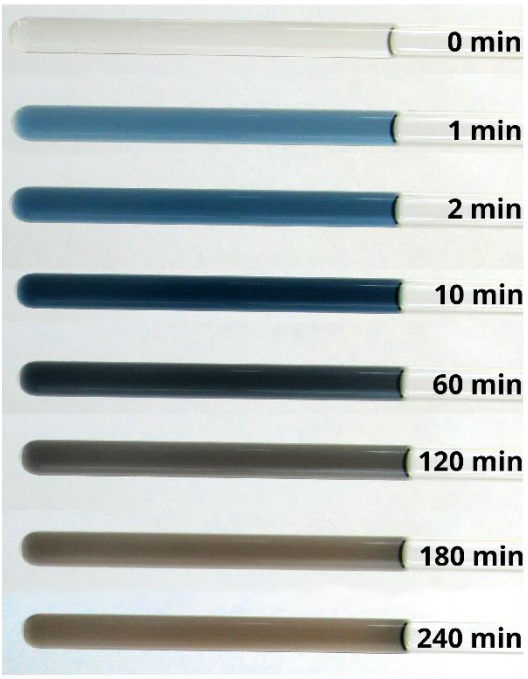
B
0 min
1 min
2 min
10 min
60 min
120 min
180 min
240 min

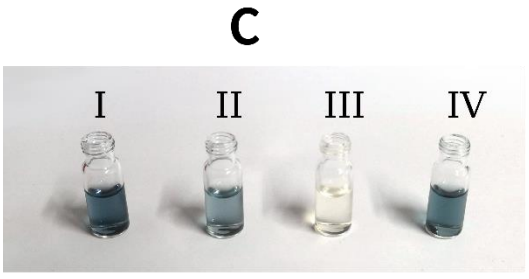
C
I
II
III
IV

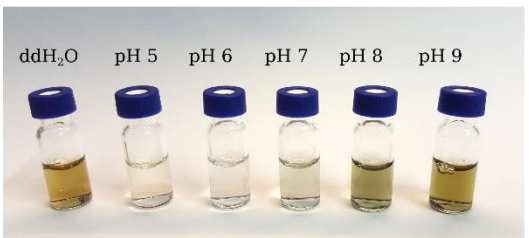
D
ddH2O
pH 5
pH 6
pH 7
pH 8
pH 9

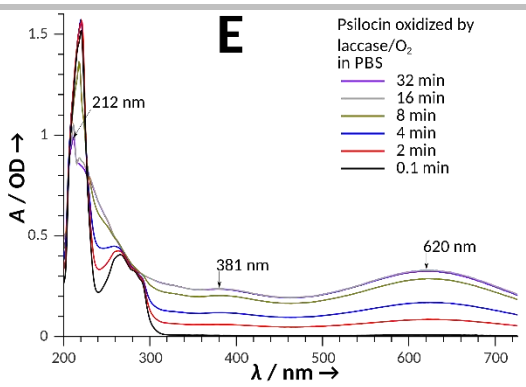
E
Psilocin oxidized by laccase/O2 in PBS
32 min
16 min
8 min
4 min
2 min
0.1 min
212 nm
381 nm
620 nm
A / OD →
λ / nm →

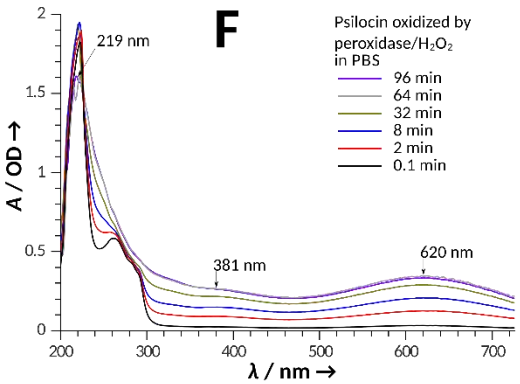
F
Psilocin oxidized by peroxidase/H2O2 in PBS
96 min
64 min
32 min
8 min
2 min
0.1 min
219 nm
381 nm
620 nm
A / OD →
λ / nm →

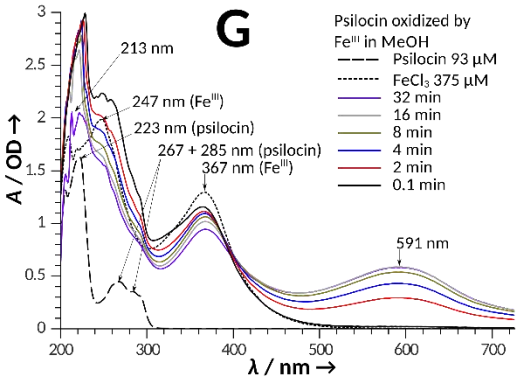
G
Psilocin oxidized by FeIII in MeOH
Psilocin 93 µM
FeCl3 375 µM
32 min
16 min
8 min
4 min
2 min
0.1 min
213 nm
247 nm (FeIII)
223 nm (psilocin)
267 + 285 nm (psilocin)
367 nm (FeIII)
591 nm
A / OD →
λ / nm →

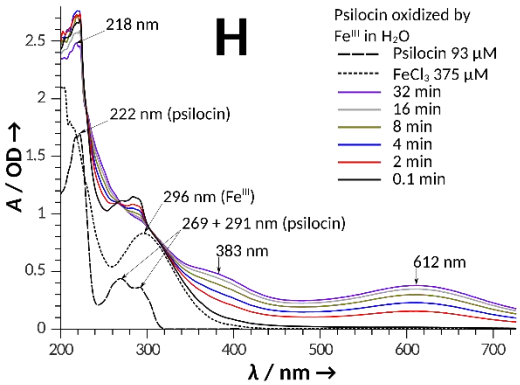
H
Psilocin oxidized by FeIII in H2O
Psilocin 93 µM
FeCl3 375 µM
32 min
16 min
8 min
4 min
2 min
0.1 min
218 nm
222 nm (psilocin)
296 nm (FeIII)
269 + 291 nm (psilocin)
383 nm
612 nm
A / OD →
λ / nm →

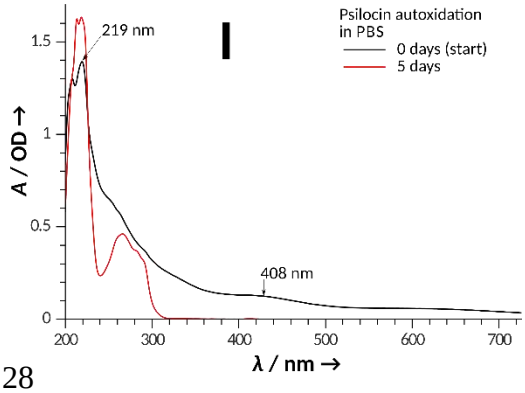
I
Psilocin autoxidation in PBS
0 days (start)
5 days
219 nm
408 nm
A / OD →
λ / nm →

Figure S10. Color development under different conditions of **2** oxidation.

A) NMR autoxidation conditions.

B) NMR peroxidase/H_2O_2 conditions.

C) Fe^{III} mediated oxidation of a dilute **2** solution in H_2O/methanol (1:1). I: 250 µM **2** and 500 µM $FeCl_3$, II: identical reaction to which 150 µM EDTA were added after 20 min, III: identical reaction with added excess EDTA after 20 min, IV: identical reaction to which excess EDTA was added after 20 min followed by re-addition of $FeCl_3$.

D) Autoxidation of 1 mM **2** in ddH_2O or Britton-Robinson buffers of varying pH after 3 d.

E) UV/Vis spectra of **2** and its oxidation products, recorded over 32 min, oxidized by laccase and O_2 in PBS.

F) UV/Vis spectra of **2** and its oxidation products, recorded over 96 min, oxidized by peroxidase and H_2O_2 in PBS.

G) UV/Vis spectra of **2** and its oxidation products, recorded over 32 min, oxidized by Fe^{III} in MeOH.

H) UV/Vis spectra of **2** and its oxidation products, recorded over 32 min, oxidized by Fe^{III} in H_2O.

I) Endpoint UV/Vis spectra of **2** autoxidation after 5 d in PBS.

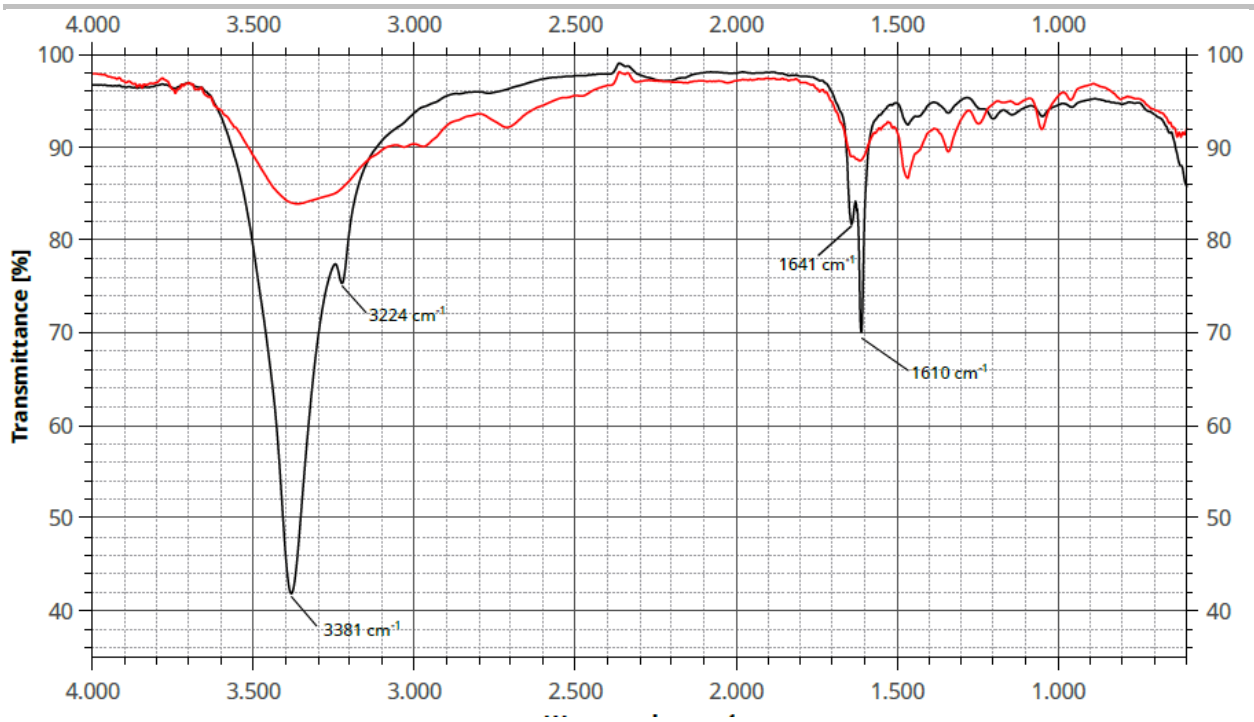

Figure S11. FT-IR spectra of blue oligomeric (black spectrum) and polymeric (red) product fractions.

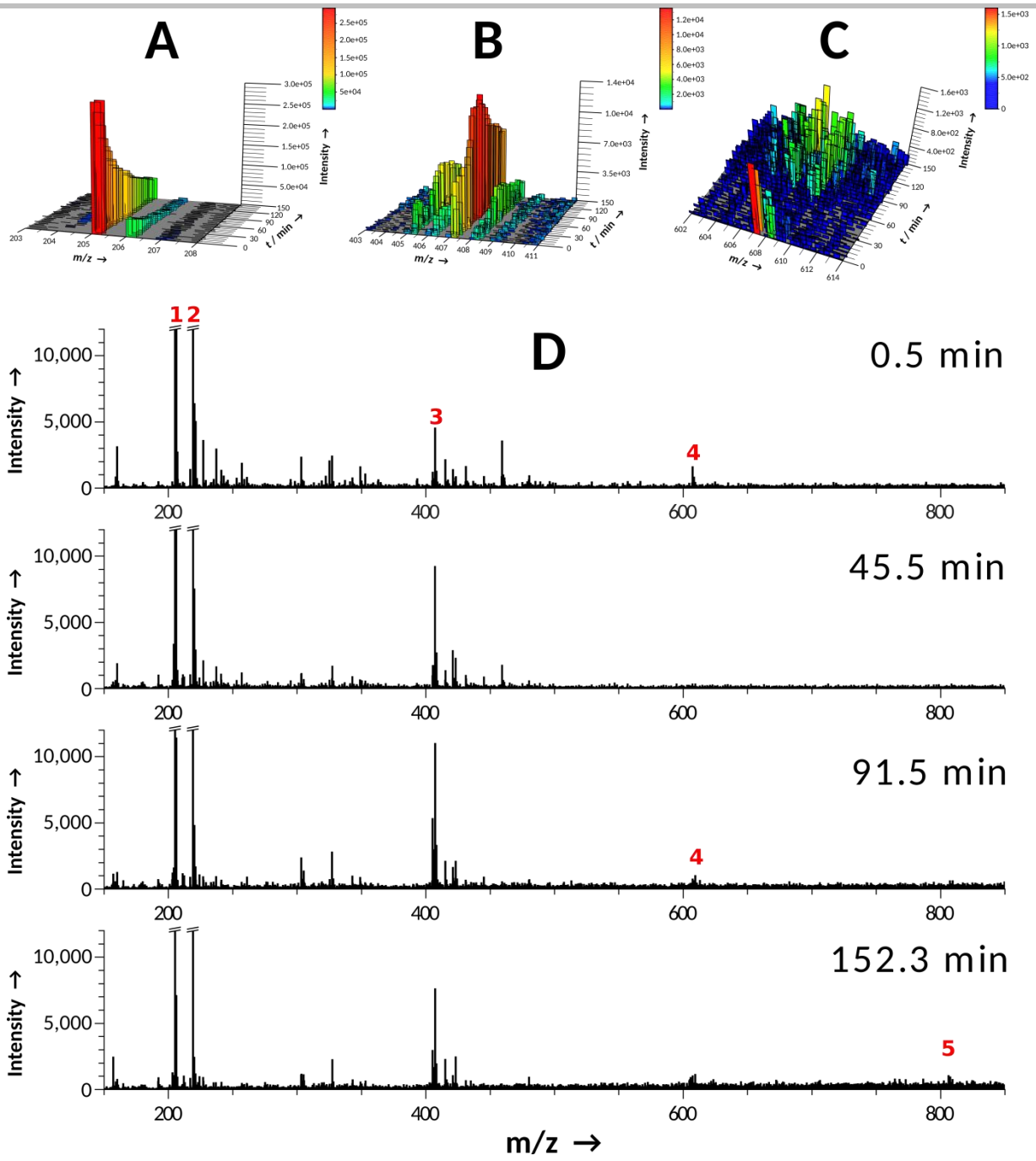

Figure S12. Time-resolved mass spectrometric analysis of **2** oxidation by the recombinant *Myceliophthora thermophila* laccase. Initial **2** concentration was 500 µM. A) Three dimensional plot of decreasing substrate concentration. B) Three dimensional plot of dimeric ion species (*m/z* 405 and 407). C) Plot of trimeric ion species *m/z* 605 to 609. D) Full spectral view of selected time points. Annotations: 1: psilocin (*m/z* 205); 2: psilocin quinone (*m/z* 219, mainly artefact due to psilocin oxidation in ESI spray chamber); 3: dimers as shown in panel B; 4: trimers as shown in panel C; 5: tetramers (*m/z* 807 to 811). Signals of **1** and **2** were cut off for better visibility of products. Note the presence of autoxidation products of **2** from the stock solution in the first spectrum, that have gradually been consumed by emerging polymers and been bound to protein within the first quarter of the reaction time.

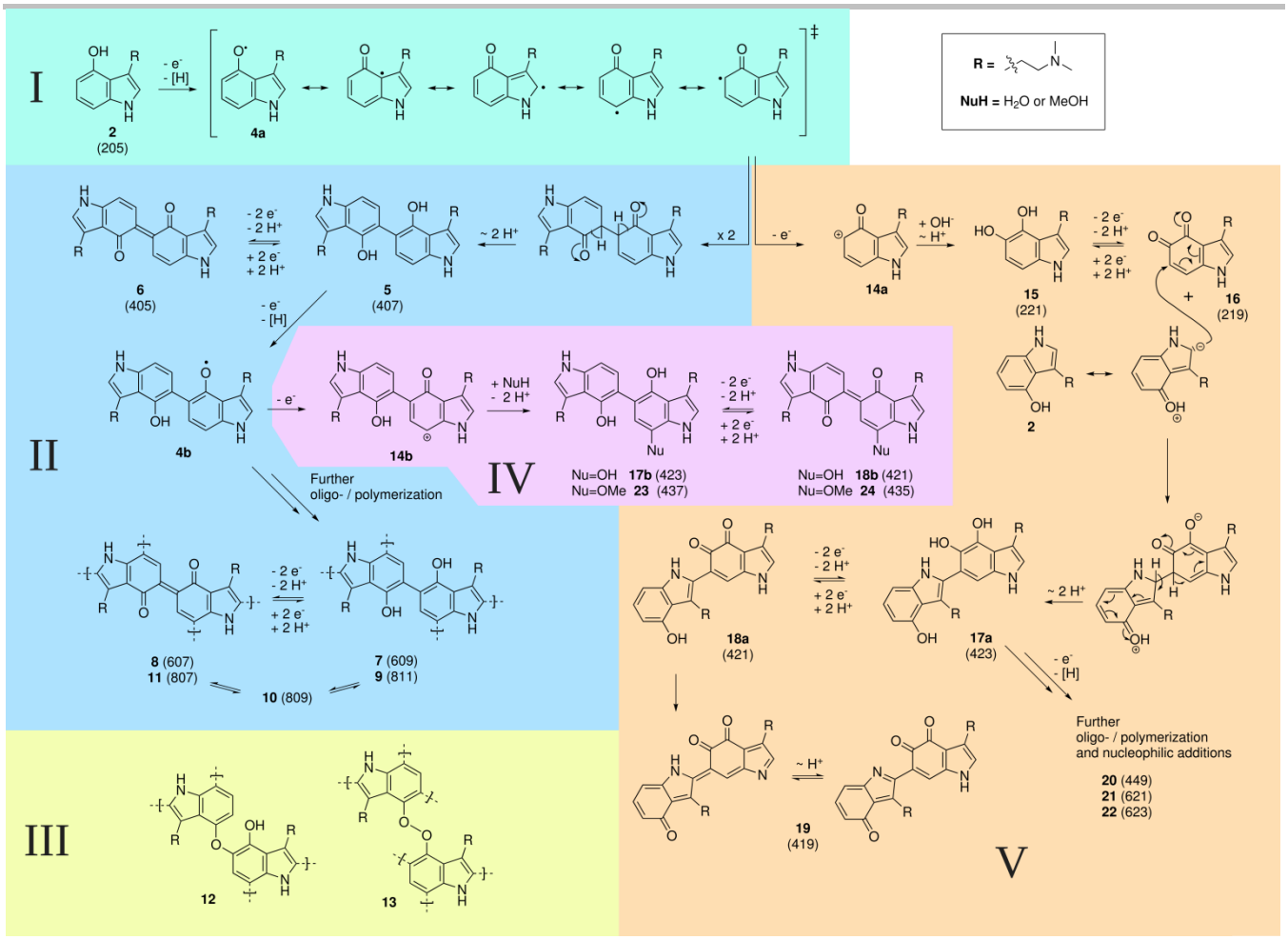

Figure S13. Plausible mechanism for formation of mass spectrometrically detected **2** oxidation products. Coupling positions are chosen based on plausibility, as suggested by NMR spectroscopy, and fundamental electronic and steric considerations. Structural isomers may occur.

I (emerald sector): Initial formation of psilocyl radical **4a** and its mesomeric forms analogous to phenol oxidation.[19,20]

II (blue sector): Radical coupling of monomers to first hydroquinoid dimer **5**, and by further oxidation via additional radical intermediates, such as **4b**, to hydroquinoid higher oligo- and polymers (**7**, **9**). Hydroquinoid moieties undergo reversible oxidation via semiquinoid forms to colored quinoid oligomers (**6**, **8**, **11**). From tetramers upwards, hybrid quinoid-hydroquinoid species, such as tetramer **10**, exist.

III (yellow sector): Besides C-C coupling, C-O-C and C-O-O-C coupling may occur to yield products **12** and **13**. Assumed instability of the latter[21] may give rise to further diversification of the product spectrum.

IV (violet sector): If the radical electron is lost, cationic oligomer **14b** may be formed,[22] which would be attacked by nucleophiles (e.g., H_2O or methanol from solvent) to give rise to additional hydroxylated or methoxylated dimers (**17b**, **23**). These may form quinoid derivatives (**18b**, **24**).

V (orange sector): Under autoxidation conditions, especially at high pH and low **2** concentrations, coupling is likely entirely based on nucleophilic additions due to small populations of **4a**. Cation **14a** would react with water or hydroxide to form 5-hydroxypsilocin **15** and subsequently *o*-indolequinone **16**. A nucleophilized carbon, e.g., the electron-rich position 2,[23] may attack the *o*-quinone to form the trihydroxylated dimer **17a**. A similar situation has been postulated for 5,6-dihydroxyindole coupling.[24] **17a** may either be oxidized to a hydroxyquinoid dimer **18a** and oxoquinoid **19**, or, by acquiring additional nucleophiles, to **20**-**22**, or to even larger products.

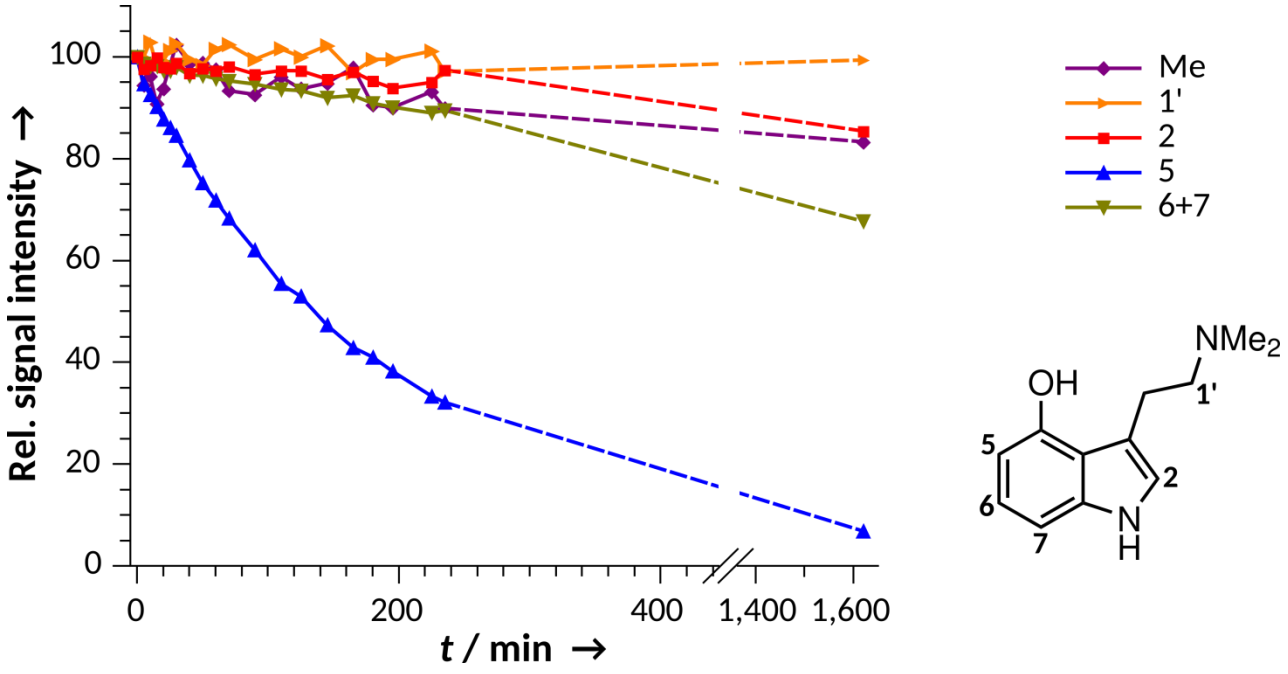

Figure S14. *In situ* ^{1}H NMR spectroscopy of **2** autoxidation. Shown is the integration of ^{1}H signals.

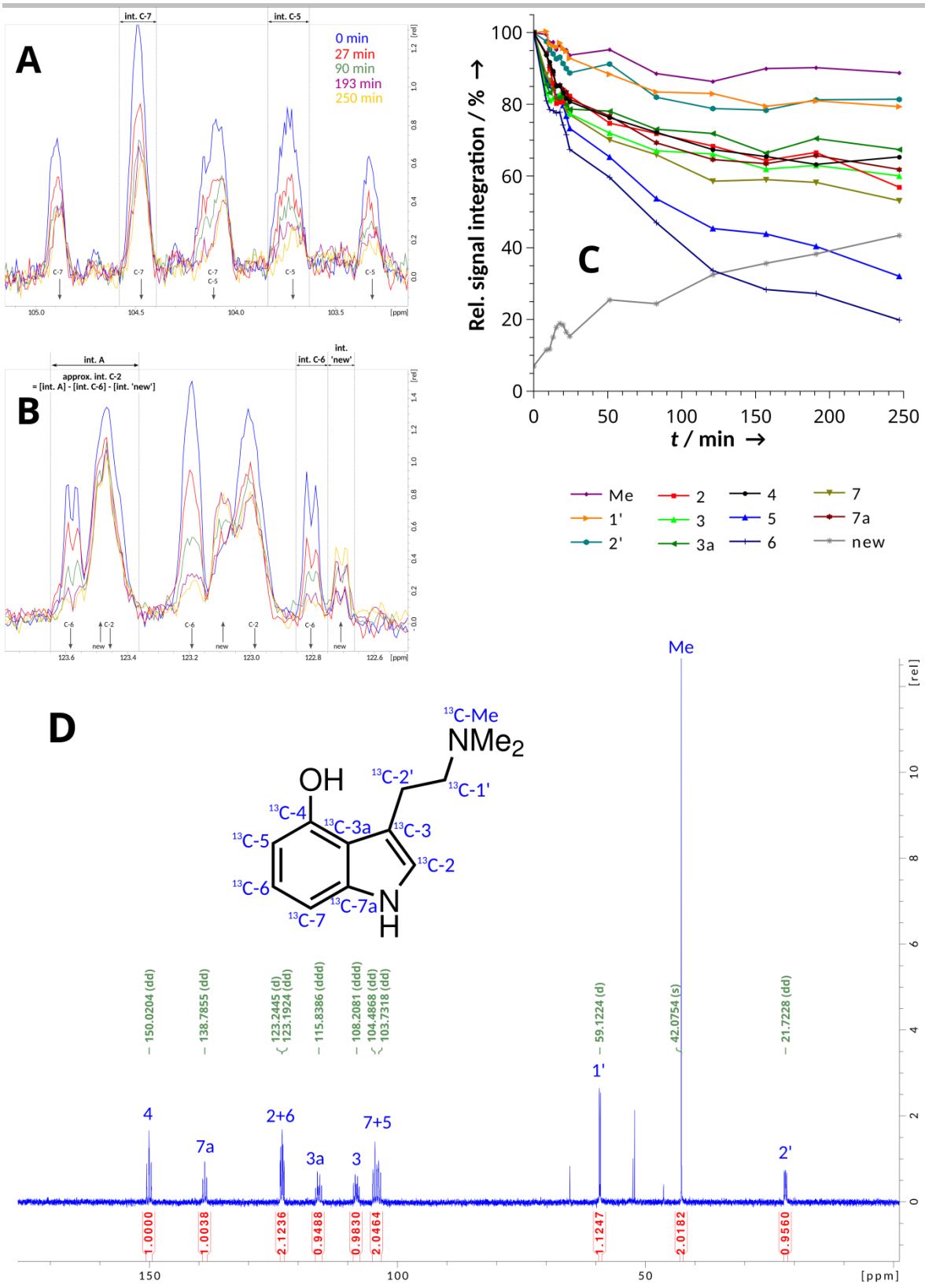

Figure S15. *In situ* inverse-gated decoupling ^{13}C NMR spectroscopy (150 MHz) of **2** oxidation, catalyzed by horseradish peroxidase and H_2O_2. A) Close-up view of signal changes of C-5 and C-7 during the reaction, and corresponding integration ranges. B) Detail of signal changes of C-2 and C-6 and emerging ("new") signal during the reaction, along with corresponding integration ranges and approximate calculations. C) Complete result chart of ^{13}C-signal changes. D) Fully annotated inverse-gated decoupling ^{13}C NMR spectrum of $^{13}C_{12}$-**2**.

References

[1] C. Lenz, J. Wick, D. Hoffmeister, *J. Nat. Prod.* **2017**, *80*, 2835-2838.

[2] S. Hoefgen, J. Lin, J. Fricke, M. Stroe, D. J. Mattern, J. E. Kufs, P. Hortschansky, A. A. Brakhage, D. Hoffmeister, V. Valiante, *Metab. Eng*. **2018**, *48*, 44-51.

[3] A. Hofmann, R. Heim, A. Brack, H. Kobel, A. Frey, H. Ott, T. Petrzilka, F. Troxler, *Helv. Chim. Acta* **1959**, *42*, 1557-1572.

[4] Z. Olempska-Beer. Laccase from *Myceliophthora thermophila* expressed in *Aspergillus oryzae*. Joint FAO/WHO Expert Committee on Food Additives, **2004**.

[5] a) J. Fricke, F. Blei, D. Hoffmeister, *Angew. Chem. Intl. Ed*. **2017**, *56*, 12352-12355; b) I. V. Grigoriev, R. Nikitin, S. Haridas, A. Kuo, R. Ohm, R. Otillar, R. Riley, A. Salamov, X. L. Zhao, F. Korzeniewski, T. Smirnova, H. Nordberg, I. Dubchak, I. Shabalov, *Nucleic Acids Res*. **2014**, *42*, D699-D704.

[6] J. Cox, M. Mann, *Nat. Biotechnol*. **2008**, *26*, 1367-1372.

[7] J. Cox, N. Neuhauser, A. Michalski, R.A. Scheltema, J.V. Olsen, M. Mann. *J. Proteome Res*. **2011**, *10*,1794-1805.

[8] O.H. Lowry, N.J. Rosebrough, A.L. Farr, R. Randall, *J. Biol. Chem.* **1951**, 193, 265-275.

[9] B. Ehresmann, P. Imbault, J.H. Well, *Analyt. Biochem*. **1973**, *54*, 454-463.

[10] R.M. Berka, P. Schneider, E.J. Golightly, S.H. Brown, M. Madden, K.M. Brown, T. Halkier, K. Mondorf, F. Xu, *Appl. Environ. Microbiol*. **1997**, *63*, 3151-3157.

[11] F. Sievers, D.G. Higgins, *Protein Sci.* **2018**, *27,* 135-145. doi: 10.1002/pro.3290. Epub 2017 Oct 30.

[12] S.F. Altschul, T.L. Madden, A.A. Schäffer, J. Zhang, Z. Zhang, W. Miller, D.J. Lipman, *Nucleic Acids Res*. **1997**, *25*, 3389-3402.

[13] M. Stanke, R. Steinkamp, S. Waack, B. Morgenstern, *Nucleic Acids Res*. **2004**, *32*, W309-312.

[14] T.N. Petersen, S. Brunak, G. von Heijne, H. Nielsen, *Nat. Methods* **2011**, *8*, 785-786.

[15] a) NetNGlyc server of the Denmark Technical University at http://www.cbs.dtu.dk/services/NetNGlyc/; b) C. Steentoft, S.Y. Vakhrushev, H.J. Joshi, Y. Kong, M.B. Vester-Christensen, K.T. Schjoldager, K. Lavrsen, S. Dabelsteen, N.B. Pedersen, L. Marcos-Silva, R. Gupta, E.P. Bennett, U. Mandel, S. Brunak, H.H. Wandall, S.B. Levery, H. Clausen, *EMBO J*. **2013**, *32*, 1478-1488.

[16] S. Negi, S. Pandey, S.M. Srinivasan, A. Mohammed, C. Guda, *Database* **2015**, pii: bav003.

[17] A.E. Kelly, H.D. Ou, R. Withers, V. Dötsch, *J. Am. Chem. Soc*. **2002**, *124*, 12013-12019.

[18] a) G.Q. Zhang, Q.J. Chen, J. Sun, H.X. Wang, C.H. Han, *J. Basic Microbiol.* **2013**, *53*, 868-875; b) E. J. Mullaney, A.H. Ullah, *Biochem. Biophys. Res. Comm*. **1998**, *243*, 471-473.

[19] M.Z. Wrona, G. Dryhurst, *J. Pharm. Sci*. **1988**, *77*, 911-917.

[20] A.N. Shendrik, I.D. Odaryuk, L.V. Kanibolotska, E.A. Kalinichenko, A.S. Tsyapalo, V.V. Beznos, *Int. J. Chem. Kinet.* **2012**, *44*, 414-422.

[21] A. Steevensz, L.G. Cordova Villegas, W. Feng, K.E. Taylor, J.K. Bewtra, N. Biswas, *J. Environ. Engin. Sci.* **2014***, 9*, 181-186.

[22] S. Yamamura, S. Nishiyama, *Synlett* **2002**, 533-543.

[23] H.C. Longuet-Higgins, C.A. Coulson, *Trans. Faraday Soc.***1947**, *43*, 87-94.

[24] M. d'Ischia, A. Napolitano, A. Pezzella, E.J. Land, C.A. Ramsden, P. Riley in *Advances in Heterocyclic Chemistry* (ed. A.R. Katritzky), Academic Press, 2005, **89**, pp1-63.